Pure & Appl. Chem., Vol.53, pp.259-286.
Pergamon Press Ltd. 1981. Printed in Great Britain.

0033-4545/81/0101-0259$02.00/0

MICELLES, MAGNETS AND MOLECULAR MECHANISMS. APPLICATION TO CAGE EFFECTS AND ISOTOPE SEPARATION.

Nicholas J. Turro

Department of Chemistry, Columbia University, New York, New York 10027

Abstract. This report reviews the general problem of cage reactions of radical pairs and diradicals. Based on Wigner's spin conservation rule and the expectation that only singlet radical pairs can undergo cage reactions, a natural consequence is the expectation that it should be possible to observe magnetic effects on the reactions of radical pairs. It is shown that two types of magnetic effects should be possible: (1) Effects due to the application of the magnetic field of a laboratory magnet during a reaction; (2) Effects due to the interactions of nuclear magnetic moments and electron magnetic moments. The experimental consequences of these magnetic effects are separation of isotopes based on differing nuclear magnetic moments and variation of the extent of cage reaction by variation of an applied field or by variation of nuclear magnetic moments. Striking experimental examples of these magnetic effects are provided by the photolysis of ketones in micellar solution and by the thermolysis of endoperoxides.

INTRODUCTION

Upon introduction to radical chemistry, the student quickly learns that radical pairs can undergo "cage" reactions that result in combination and disproportionation of the radical fragments. Later he discovers that when the radical pair exists on a connected sequence of atoms, (i.e., the radical pair is a diradical) the intramolecular analogues of combination and disproportionation can also occur. Everything is readily understood in terms of "two dot" chemistry in which "dots" interact with each other to form bonds (combination) or in which "dots" interact with hydrogen atoms next to radical centers to form two new molecules (disproportionation). Often, in a separate course on quantum mechanics, the student may discover that the two dots have a detailed electronic structure that was not explicitly considered when the chemistry of radical pairs was discussed. Ideas such as electron spin correlation, triplet radical pairs, singlet radical pairs, and doublets come up and the question arises: Do these ideas have any relationship to the two dot chemistry of radical pairs and diradicals? In a course on magnetic resonance and in reading the research literature, the student may learn that the odd electron of radicals interact with magnetic nuclei and that funny NMR spectra (CIDNP) sometimes arise when reactions involving radicals are analyzed in a NMR spectrometer. Again a question arises: Are these spectroscopic phenomena related in any chemically significant manner to the two dot chemistry of radical pairs and diradicals?

Many students who do research involving two dot chemistry occasionally get into extensive discussions of the problem of how a radical pair, just born as a triplet (two parallel electron spins) can become a singlet radical pair (one electron spin up and one electron spin down). How do such "spin flips" occur? What does it mean to separate the "correlated" triplet dots in space to "infinity" and thereby lose the correlation?

In this report we shall attempt to show how an understanding of two dot chemistry indeed requires an integration of concepts such as electron spin correlation, electron-nuclear interactions and magnetic resonance. This integration allows the rational design of remarkable experiments in which radical reactions provide a means of spontaneously sorting nuclear isotopes based on differing nuclear magnetic moments and in which the yields of products may be controlled by nuclear magnetic moments or by applications of magnetic fields comparable to those available in small laboratory magnetic stirrers. It shall be demonstrated that these effects arise as a result of the competition between cage reactions of radical pairs and irreversible escape of radical pairs from cages. These effects will be shown to be enhanced when the cages holding the radical pairs are the hydrophobic cores of micellar aggregates. Finally, it will be demonstrated that such effects are not confined to micellar systems, but that they also occur in thermal reactions.

SOME FUNDAMENTAL RULES

Several useful rules shall serve as guides to understanding the mechanisms of reactions of radical pairs produced by homolytic cleavage of a typical organic molecule:

Rule 1. (Wigner's spin conservation rule). When the bond connecting two groups a and b undergoes homolytic cleavage, the radical pair (å,b̊) is produced with conservation of spin of the immediate precursor. This means that homolytic cleavage of a singlet molecule ^{1}a-b will produce a singlet radical ^{1}(å,b̊) and that homolytic cleavage of a triplet molecule ^{3}a-b will produce a triplet radical pair, ^{3}(å,b̊).

^{1}a-b → ^{1}(å,b̊) singlet molecule → singlet radical pair

^{3}a-b → ^{3}(å,b̊) triplet molecule → triplet radical pair

Rule 2. Singlet radical pairs can undergo "two-dot" cage reactions of combination and disproportionation which lead to molecular products, but triplet radical pairs cannot undergo such cage reactions. This means that a triplet radical pair must undergo intersystem crossing (ISC) to a singlet radical pair before it can undergo a cage reaction.

^{1}(å,b̊) → cage combination or cage disproportionation

^{3}(å,b̊) —ISC→ ↑

From these rules it can be seen that an understanding of the mechanisms for ISC of a triplet radical pair is required for an understanding of the two dot chemistry of triplet radical pairs. The latter are commonly produced in many important photoreactions, including most reactions of n,π* states.

MAGNETIC EFFECTS ON ORGANIC REACTIONS

We shall demonstrate that as a natural consequence of the two rules listed in the previous section, magnetic field and magnetic isotope effects are expected to occur in reactions involving radical pairs. The possibility that the reactivity and efficiency of reactions involving radical pairs will depend on nuclear spin states (or laboratory magnetic fields) is a rather fascinating idea in view of the tiny interactions that exist between electron spins and nuclear spins (or electron spins and laboratory magnetic fields). Many chemists are accustomed to thinking of nuclei as passive mass points, whose inertia only allows them to follow but not to influence electronic processes in a significant way (1). However, in addition to mass, nuclei possess a second important property (or non-property): Magnetism or magnetic spin (or diamagnetism or lack of magnetic spin). The latter property is not usually considered in a discussion of reaction mechanisms. Nevertheless, the influence of substitution of ^{13}C (magnetic, spin 1/2) for ^{12}C (non-magnetic, spin 0) or of ^{2}H (magnetic, spin 1) for ^{1}H (magnetic, spin 1/2) or of ^{17}O (magnetic, spin 5/2) for ^{16}O or ^{18}O (non-magnetic, spin 0) could lead to net chemical effects that are due to the magnetic, rather than to the mass properties of nuclei. Similarly, the possible influence of laboratory magnetic fields on chemical reactions represents an intriguing notion but most chemists would be hard pressed to cite any famous, documented cases (or even any obscure, undocumented examples) (2).

A simple thermodynamic argument has been employed to summarily dismiss any serious possibility of significant magnetic field or magnetic isotope effects on the rates and/or efficiencies of chemical processes. The logic goes as follows. As shown in Table 1, the strongest laboratory magnetic fields (∿100,000 Gauss) correspond to tiny energies (∿0.03 kcal/mole) relative to the commonly encountered activation energies of chemical reactions (30 kcal/mole). Hence, neither laboratory nor nuclear magnets can be expected to produce measurable effects on the energetics of chemical processes. Hence, there can be no serious possibility of magnetic field effects or magnetic isotope effects on chemical processes. This is a pretty good argument, as far as it goes, and it would be difficult to refute if the rates and efficiencies of chemical reactions depended only on energetic considerations.

Reaction rates and efficiencies depend not only on energetic factors but also depend on entropic factors. The latter correspond to the molecule's "getting it all together" when it possesses the correct amount of energy and being able to "do it" within a narrow window of time. In terms of the Arrhenius formulation of rates, a rate constant is given by $k = A\, e^{-\Delta E/RT}$. The "A-factor" may be viewed as a measure of how tough it is to "get it all together" at the molecular level when the energy and the time are "just right". Magnetic effects on the A factor are possible if "getting it right" means interconverting states that possess different

magnetic properties, i.e., triplet states and singlet states.

TABLE 1. Conversion table of magnetic field effects.

	Gauss	cm^{-1}	kcal/mole
very strong magnet	100,000 G	10 cm^{-1}	10^{-2} kcal/mole
strong magnet	10,000 G	1 cm^{-1}	10^{-3} kcal/mole
toy magnet, strong hf	100 G	10^{-2} cm^{-1}	10^{-5} kcal/mole
typical hf	10 G	10^{-3} cm^{-1}	10^{-6} kcal/mole
earth's magnetic field	1 G	10^{-4} cm^{-1}	10^{-7} kcal/mole
chemical bond	$2x10^{8}$ G	20,000 cm^{-1}	59 kcal/mole

For example, if a rate or efficiency limiting step of a reaction sequence is a triplet-singlet intersystem crossing, a mechanism involving magnetic interactions is automatically required. In such a situation the magnetic spin properties of nuclei, by controlling the rate of intersystem crossing, may determine the reactivity and efficiency of certain reaction pathways.

When a molecule undergoes a homolytic cleavage, a radical pair is produced, two free radical centers are formed and large magnetic moments are created. It is therefore natural to search for magnetic effects in the chemistry of radical pairs. We now give a brief, qualitative description of the origins of magnetic effects on the reactivity of radical pairs.

Spin correlated and spin random radical pairs.
The ability of a radical pair to undergo a cage combination or a cage disproportionation reaction depends on the electronic spin state of the radical pair. In general, a caged radical pair may be characterized as existing in one of three states: singlet state, triplet state, and two doublet states. The electron spins of the radical pair are correlated in the singlet

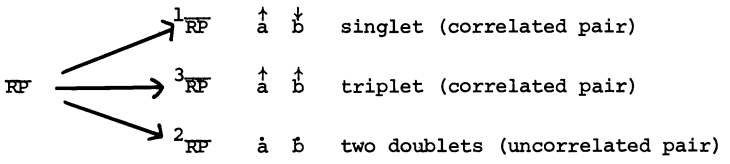

state and in the triplet state, but are uncorrelated when both radicals are doublets. The correlation of spins in the singlet and triplet states may be visualized by use of a vector model (Fig. 1). (4)

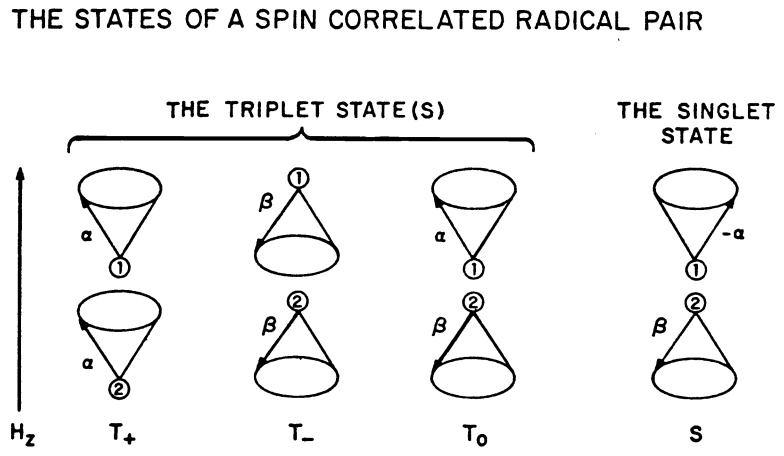

Fig. 1 Vector model of the triplet and singlet states of a radical pair (or diradical). The direction of an arbitrary magnetic field H_z is used as an orienting directing direction about which the electron spin vectors precess.

For the two odd electrons of the radical pair, quantum mechanics allows four possible arrangements of the electron spin vectors (relative to some defined magnetic field axis H_z determined by the strongest magnetic interactions experienced by the spins). The spin vectors must point in the direction of H_z (α spins) or in a direction opposite to H_z (β spins). Next it is noted that the four allowed arrangements of spins are $\alpha\alpha$, $\beta\beta$, $(\alpha\beta)_+$ (in phase) and $(\alpha\beta)_-$ (out of phase). The $\alpha\alpha$, $\beta\beta$,and $(\alpha\beta)_+$ arrangements comprise the three components of a (spin correlated) triplet radical pair whereas the $(\alpha\beta)_-$ arrangement corresponds to a (spin correlated) singlet radical pair. The "correlation" of the spins is preserved as long as electron exchange is strong enough to overcome dephasing and spin vector inversions that are induced by magnetic forces experienced by the radical pair. As the fragments of the pair separate further and further from one another, the exchange interaction decreases until the spins lose their initial correlation. This means that random fluctuating magnetic fields due to electronic orbital motion or nuclear magnetic moments can cause intersystem crossing by "rephasing" of singlet radical pairs to triplet radical pairs, as shown in Fig. 2, i.e., S $(\alpha\beta)_- \rightarrow$ T $(\beta\beta)$. Conventionally, the three sublevels of a radical pair are given the following symbols: T $(\alpha\beta)_+ = T_o$, T $(\alpha\alpha) = T_+$, and T $(\beta\beta) = T_-$. The triplet sublevels are all characterized by a net spin angular momentum of unity (spin multiplicity, S = 1), and by a quantum number M_S (+1, 0, -1) which characterize the T_+, T_o and T_- levels, respectively.

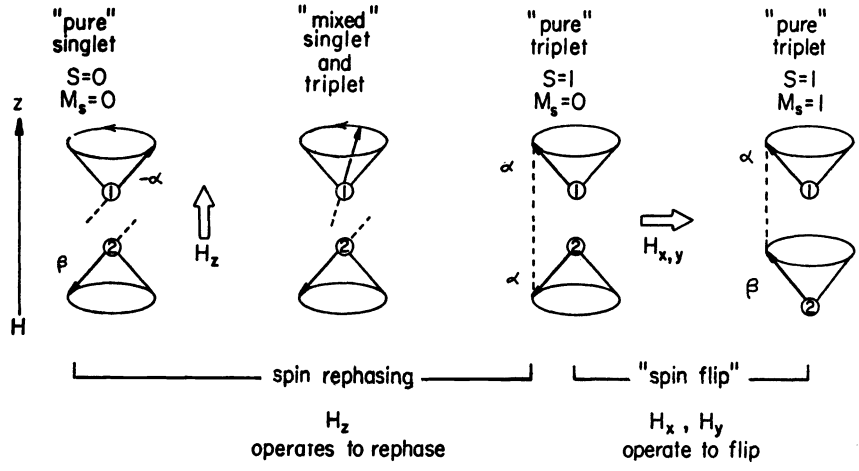

Fig. 2 Schematic vector representation of two mechanisms for intersystem crossing in a radical pair. In the first mechanism, $T_o \not\gtrless S$, a magnetic field (due to a laboratory field or a nuclear magnetic moment) in the z direction causes the two electron spin vectors (initially $-\alpha\beta$) to precess about H at different frequencies. It is the relative precessional rate which matters here. In the fig. the $-\alpha$ spin is shown undergoing "spin rephasing" as it switches from a-α to an α orientation, converting a singlet ($-\alpha\beta$) to a triplet ($\alpha\beta$). In the second mechanism, $T_+ \not\gtrless S$, a nuclear moment causes a torque on the electron spin in the x (or y) direction and causes an electron spin flip ($\alpha \rightarrow \beta$) which occurs simultaneously with a nuclear spin flip.

Electron exchange and Zeeman interaction. Splitting of triplet sublevels and splitting of singlet and triplet states.

We shall now consider two interactions which "split" energy levels and in doing so, can inhibit certain ISC mechanisms relative to others.

The first interaction is the exchange of odd electrons of the radical pair which is characterized by an exchange energy, J. The exchange interaction is electrostatic (non-magnetic) and is distinguished from Coulombic interactions by its dependence on electron spin, i.e., spin dependent exchange electrostatic forces must be postulated as a fundamental principle of quantum mechanics. As we have seen earlier, the two odd electrons of a radical pair may be oriented (in a magnetic field) so that their magnetic vectors may be either added or subtracted to yield a total spin of unity (triplet state) or zero (singlet state). The exchange interaction causes the energies of the singlet and triplet state to differ by the quantity, J. The greater the exchange of electrons the greater the value of J and the larger the energy separation of S and T. The magnitude of J drops off rapidly as one proceeds from a bonded pair of nuclei (J$\sim$60-80 kcal/moles) to a caged radical pair (Figure 3).

The exchange interaction may be viewed as a force that tends to preserve an initial spin orien-

tation. In other words, in an electron exchange, all quantum numbers remain identical, so that electron spin multiplicity cannot change during an electron exchange, unless a force whose energy is stronger than J operates during the exchange process.

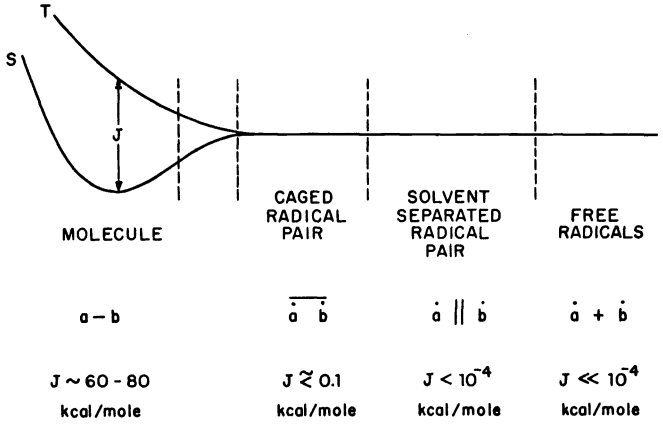

Fig. 3 Schematic representation of the exchange interaction, J, of an electron pair initially localized in a bond between groups a and b and then localized as odd electrons on a and b. The effect of J is to energetically split $T_{\pm}$ and T_0 from S and thereby inhibit ISC.

The second interaction is that between the electron spins and local magnetic forces due to macroscopic laboratory magnetic fields and to microscopic magnetic fields due to electron spins and nuclear spins. The Zeeman interaction refers to the interaction of electron spins with a macroscopic magnetic field and is responsible for the splitting of the T_+, T_0 and T_- levels in a laboratory field (Fig. 4). Note that the magnitude of the splitting is equal to $g\beta\vec{H}$ where g is the g-factors (available from ESR spectroscopy) of radicals a and b, and β is Bohr magneton, a fundamental constant for electrons.

From the above discussion it is clear that magnetic forces cannot compete with exchange forces until the radical pair is well separated in space (~8-10Å).

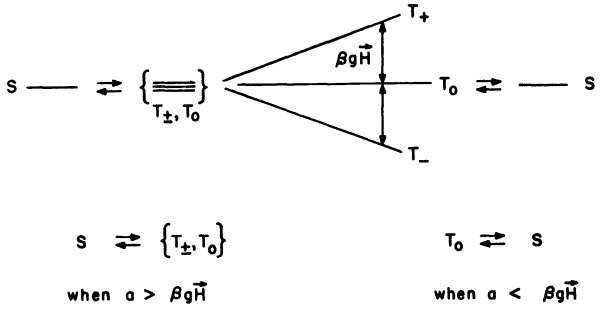

Fig. 4 Schematic representation of the Zeeman interaction $\beta g\vec{H}$ on the energetic separation of T_+, T_- and T_0. When the Zeeman interaction is small relative to other interactions (such as the hyperfine interaction whose strength is given by a, the hyperfine splitting constant), the triplet and singlet states are energetically degenerate and all three triplet sublevels interconvert with the singlet state. When $\beta g\vec{H}$ is large relative to a, only $T_0 \rightleftarrows S$ intersystem crossing occurs. The effect of $\beta g\vec{H}$ is to energetically split $T_{\pm}$ from S and thereby inhibit intersystem crossing from or to these sublevels.

The mechanisms for intersystem crossing in a radical pair.

We examine in more detail the mechanisms by which intersystem crossing may occur in a spin correlated radical pair and how the exchange and Zeeman splitting can influence intersystem crossing in radical pairs. It is useful to classify intersystem crossing (ISC) mechanisms in terms of the major interactions which cause the electron spins to rephase ($S \rightleftarrows T_0$) or to flip ($S \rightleftarrows T_+$ or $S \rightleftarrows T_-$): (1) spin orbit interaction; (2) Zeeman interaction; (3) electron-nuclear

hyperfine interaction. The spin-orbit interaction occurs because a magnetic field is generated as the result of the orbital motion of electrons and this magnetic field influences the magnetic moment due to electron spin. Let us term the rate constant for ISC by this mechanism as k_{SO}. Spin-orbit interaction is most important when the interacting electrons are on a single atomic nucleus, which is not the case in radical pairs. Thus, spin-orbit coupling is generally not an important mechanism for ISC of radical pairs.

The Zeeman interaction in addition to "splitting" T_+ and T_- away from T_o, also causes the electron spin vectors to precess about the applied field at a rate that is proportional to $\Delta g\vec{H}$ (Fig. 2). This means that because of an imbalance of g factors ($g_a \neq g_b$) the rate of the "rephasing" interconversion of T_o to S (and of S to T_o) is thus proportional to $\Delta g\vec{H}$. Let us term the rate constant for ISC by this mechanism $k_{\Delta g}$.

The electron-nuclear hyperfine interaction (hfi) is characterized by a quantity a, the hyperfine constant, which may be extracted from ESR spectrscopy. As a result of this magnetic interaction electron spins precess faster, and a ISC mechanism is thereby providing for the rephasing $S \rightleftarrows T_o$ (Fig. 2). Let the rate constant for ISC by this mechanism by k_o^a. In addition, nuclear spins may exchange momentum with electron spins via this interaction. If the nuclear spin responsible for the hfi is 1/2, then ISC processes T_+ $(-1/2) \rightleftarrows S(+1/2)$ and $T_-(-1/2) \rightleftarrows S(+1/2)$ are allowed (Fig. 2) if the energy separation of T_+, T_- and S are smaller than the hyperfine interaction. Let the rate constant for ISC by this mechanism by $k_{\pm}^a$.

In summary, three mechanisms exist for ISC of spin correlated radical: spin orbit coupling, Zeeman interaction and hyperfine interaction. The observed rate constant (k_{OB}^{ISC}) for ISC in a spin correlated radical pair is thus given by

$$k_{OB}^{ISC} = k_{SO} + k_{\Delta g} + k_o^a + k_{\pm}^a$$

When exchange interaction is largest (caged radical pair), k_{OB}^{ISC} is expected to be minimal because a large J inhibits ISC by any mechanism (Fig. 3). In a solvent separated radical pair, however, $T_{\pm}$ and T_o become degenerate with S (Fig. 3), weak magnetic interactions due to hyperfine coupling can begin to cause ISC in the radical pair. As mentioned above, k_{SO} is negligible for carbon centered radical pairs so that

$$k_{OB}^{ISC} \sim k_{\Delta g} + k_o^a + k_{\pm}^a$$

We are now in a position to perceive three limiting situations (Fig.5) for ISC in a solvent separated, spin correlated radical pair:

I. $\vec{H} = 0$ and $a \neq 0$, therefore $k_{\Delta g} = 0$ and $k_{OB}^{ISC} = k_o^a + k_{\pm}^a$

II. $\beta g\vec{H} > a > \beta\Delta g\vec{H} > 0$, therefore $k_{OB}^{ISC} = k_o^a$

III. $\beta\Delta g\vec{H} >> a$, therefore $k_{OB}^{ISC} = k_{\Delta g}$

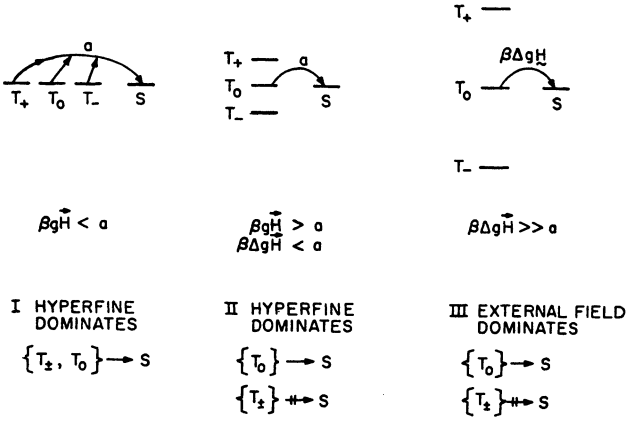

Fig. 5 Representation of the three limiting cases for ISC in an organic radical pair. In cases I and II the hyperfine interaction (a) induces ISC. In case I, all three levels participate in ISC. In case II, only T_o can undergo ISC. In case III, ISC is induced by the Zeeman interaction.

Thus, magnetic effects on radical pairs will arise whenever ISC falls into one of the limiting cases I, II or III. The chemical consequences of these limiting cases are now examined.

Chemical consequences of magnetic effects in radical pairs.
From eqs. I-III it follows that the rate of ISC of a spin correlated radical pair and hence the probability of cage reaction of a spin correlated radical pair depends both on the nuclear spins that are associated with the radical pair and on the laboratory magnetic fields experienced by the pair. The consequences of these magnetic effects on ISC are (1) a non-equilibrium population (polarization) of nuclear spin levels may be produced in the reaction products. This polarization may be determined experimentally by NMR analysis of the reaction and observation of "enhanced" absorption or enhanced "emission" of the products eventually produced by the radical pair. The phenomenon of polarization of nuclear spin level in the molecules generated from radical pairs is termed chemically induced dynamic nuclear polarization (CIDNP), and has been the subject of intense research ever since its discovery in 1967 (3); (2) Isotope effects which depend on differences in nuclear magnetic moments (magnetic isotope effects) may be observed in the rates of cage reactions of a correlated radical pair, since nuclei of different isotopes generally possess different magnetic moments and therefore exert different hyperfine interactions on electron spins. For example (Table 2) although both H and D are magnetic nuclei, H possesses a magnetic moment that is several times larger than D. As a result, for chemically equivalent positioning in a radical pair, H will induce ISC faster than D. Isotope effects can be most pronounced when comparing a magnetic isotope with a non-magnetic isotope of the same element. As seen in Table 2, ^{12}C nuclei possess no nuclear spin and therefore possess no nuclear magnetic moment, whereas ^{13}C nuclei are magnetic. As a result for chemically equivalent positioning in a radical pair, ^{13}C nuclei can induce ISC by a mechanism (hfi) that is completely unavailable to ^{12}C nuclei. The most convincing demonstration of a magnetic isotope effect would involve the unique behavior of a

TABLE 2. Some properties of common isotopes.

Nucleus	γ(a)	μ_N(b)	I (spin)	Natural abundance (%)
^{1}H	27,000	2.8	1/2	100
^{2}H	4,100	0.86	1	0.016
^{12}C	0	0	0	100
^{13}C	7,000	0.70	1/2	1.08
^{16}O	0	0	0	100
^{17}O	-3,600	-1.9	5/2	0.04
^{18}O	0	0	0	0.20

(a) Magnetogyric ratios in radians S^{-1} G^{-1}. Ref: J.E. Wertz and J.R. Bolton, "Electron Spin Resonance", McGraw-Hill, New York, 1972.
(b) Nuclear magnetic moment. Ref. M. Bersohn and J.C Baird, "An Introduction to Electron Magnetic Paramagnetic Resonance," W.A. Benjamin, New York 1966, p. 87. Units erg/G. The magnetic moment is related to the magnetogyric ratio by the relation $\mu_N = \hbar I \gamma_N$.

"middle" isotope on the rate of reaction. For example (Table 2) ^{17}O is a magnetic "middle" isotope that is flanked by non-magnetic isotopes ^{16}O and ^{18}O. As a result, if a reaction rate was special for ^{17}O relative to both ^{16}O and ^{18}O, the operation of a magnetic isotope effect would be strongly indicated. (3) The dependence of cage reaction probability on magnetic moments provides a means for the selective separation of magnetic isotopes from non-magnetic isotopes. For example, triplet radical pairs possessing magnetic nuclei will undergo faster ISC than equivalent triplet radical pairs that do not possess magnetic nuclei. As a result, cage reactions involving triplet radical pairs may produce products that are enriched in magnetic nuclei (of nuclei having larger magnetic moments). (4) The efficiency of cage reactions may depend on the strength of an external magnetic field. From Fig. 5 we see that the magnetic field effect on correlated radical pairs may arise from two different mechanisms, but that both are related to the Zeeman interaction. The first mechanism involves a simple energy splitting of the triplet sublevels. When the extent of this splitting is larger than the magnitude of the hfi, the rate of ISC from the T_+ and T_- levels is decreased. For illustration, the efficiency of hyperfine induced ISC of spin correlated triplet pair will be decreased in the presence of a magnetic field for which $\beta g\vec{H} > a$. As a result, the efficiency of cage reaction of the triplet pair will decrease.

If the external field is large enough or if Δg is large enough, the magnitude of $\beta\Delta g\vec{H}$ will be greater than the magnitude of the hyperfine interaction. Thus, in a triplet radical pair, $T_+ \rightarrow S$ and $T_- \rightarrow S$ will be negligible, but the rate of $T_o \rightarrow S$ transitions will be increased to a value larger than that at low fields. As a result, the efficiency of cage reaction of the triplet radical pair may increase in a strong enough magnetic field, after an initial decrease in weaker fields. (5) Magnetic effects on cage reactions should be possible by application of magnetic fields of the order of ∿100-500 Gauss, since even at such "weak" fields $\beta g\vec{H}$ is comparable or larger than typical values for organic radical pairs. This consequence is particularly striking because it stresses that magnetic field effects should be sought with weak fields and not only with extremely strong fields.

The role of intersystem crossing in the cage reactions of spin correlated radical pairs. According to Wigner's Spin Conservation Rule, the total electron spin of a reacting system is conserved in any elementary chemical step. The physical basis of this rule is the general lack of mechanisms for changing spin momentum during the very short lifetime of a transition state. Thus, according to Wigner's rule, only singlet radical pairs can undergo cage recombination and cage disproportionation to yield singlet molecular products. Accordingly, a triplet radical pair cannot undergo cage reaction until it has undergone ISC. However, the triplet radical pair is not prevented from undergoing processes which preserve triplet character. For example, mechanical processes such as translational displacement, conformational changes and reactions which produce a new triplet radical pair are not forbidden by Wigner's rule. As a result, ISC from a triplet radical pair to singlet radical pair, a process which requires a change in magnetic properties, will compete with other processes which preserve the initial magnetic properties (4).

Figure 6 summarizes a common situation in which translational diffusion of the fragments of a radical pair competes with ISC. Suppose after photoexcitation a molecule forms a molecular triplet, T_1, which then undergoes homolytic cleavage to produce, according to Wigner's rule, a caged triplet radical pair $^3\overline{RP}$. Hyperfine mixing does not occur effectively in the cage because J is too large. Upon formation of a solvent separated pair hfi ISC may occur to produce a singlet radical pair, $^1\overline{RP}$. The latter is expected to undergo cage reactions, with close to unit efficiency.

Let the efficiency of cage reaction starting from $^3\overline{RP}$ be $^3\Phi_{cage}$. This quantity is determined by the relative rates of ISC ($^3\overline{RP} \rightarrow {}^1\overline{RP}$) and (irreversible) diffusional separation to form (scavengable) free radicals. Let the rate constant for the $^3\overline{RP} \rightarrow {}^1\overline{RP}$ process be k_{TS} and the rate constant for irreversible diffusion separation be k_{DIF}. Then

$$^3\Phi_{cage} = \phi \frac{k_{TS}}{k_{TS} + k_{DIF}} \qquad (1)$$

where ϕ is the efficiency of formation of ^3RP. From eq. 1 it is clear that since k_{TS} may be influenced by magnetic effects, then $^3\Phi_{cage}$ may be influenced by magnetic effects, also.

We now present a highly simplified but physically reasonable and insightful model for understanding how cage effects of radical pairs originate and why they are especially prone to the influence of magnetic effects.

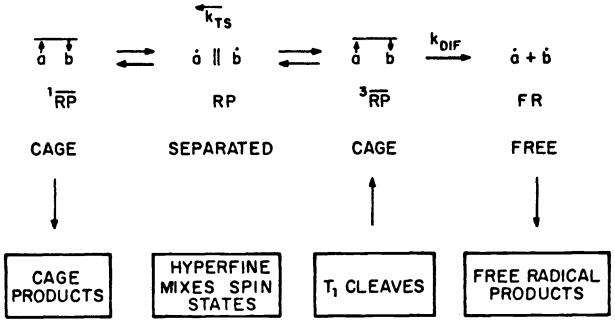

Fig. 6 Generation of a triplet radical pair from a triplet (T_1) molecule precursor. After formation of the caged primary triplet radical geminate pair $^3\overline{RP}$, a competition between cage reaction (which requires a prior ISC) and translational diffusion of the radical fragments develops.

Molecular mechanics. Solvent cages and the reactions of radical pairs. A mechanical picture of the effect of a solvent cage on chemical reactivity was recognized by Frank and Rabinowitch (5). These authors suggested that if two particles encounter and become

nearest neighbors in the solution phase, the solvent molecules surrounding the particles constitute a mechanical "cage". The latter inhibits (relative to the gas phase) the translational separation of the encounter pair. The cage causes collisions of an encounter pair to occur in sets, estimated to be of the order of 10-100 for small molecules in non-viscous solvents. The basis of the increase in collisions is the requirement that one of the two particles, after undergoing a collision with its encounter partner, must find a "hole" in the walls of the solvent cage that is large enough to provide an egress for "escape" from the solvent cage. The absence of such a hole will cause a reflection of the particle back into collision with its partner. The sequence-collision, search for an escape egress, reflection, collision- will continue until either a reaction has occurred or escape occurs.

Noyes (6) elaborated the cage model by recognizing that particles which have just escaped from a solvent cage may have a high probability of reencountering their original partner, i. e., the probability of return to the cage is competitive with irreversible escape.

These ideas of solvent cages have had a considerable impact on the interpretation of the chemistry of radicals which are commonly generated from precursor molecules in pairs. Consider a caged radical pair $\overline{\dot{a}\ \dot{b}}$ that is produced in solution as the result of homolytic cleavage of a precursor molecule a-b. We term $\overline{\dot{a}\ \dot{b}}$ a primary geminate caged radical pair, where primary refers to the facts that the pair was produced directly from a molecular precursor, and that neither partner has yet escaped the initial cage in which the pair was born, and geminate refers to the fact that both $\dot{a}$ and $\dot{b}$ possess a common parentage and are offspring of the same precursor molecule. In time, either $\dot{a}$ or $\dot{b}$ will find a hole in the wall of the solvent cage and produce a solvent separated geminate pair $\dot{a}\,\|\,\dot{b}$. The latter pair may either reencounter and produce a secondary, geminate caged pair, $\overline{\overline{\dot{a}\ \dot{b}}}$ or undergo further diffusional separation and (eventually) achieve a random separation in the solution, i.e., the geminate pair becomes two free radicals $\dot{a} + \dot{b}$.

Figure 7 summarizes the processes discussed above. Suppose we now consider the reactions and processes of a caged pair $\overline{\dot{a}\ \dot{b}}$. In general, these cage processes may be classified as (1) combination reactions; (2) disproportionation reactions; (3) chemical modification, e.g., reactions which convert $\overline{\dot{a}\ \dot{b}}$ into a chemically modified radical pair and (4) physical modification e.g., spin state interconversions.

Notice that cage processes may occur from an $\dot{a}$ radical and a $\dot{b}$ radical of three types: (1) from primary geminate pairs; (2) from secondary geminate pairs and (3) from pairs formed from free radicals that have previously achieved random separation in solution. Cage processes of types 1 and 2 lead exclusively to combination and disproportionation reactions of fragments originating from the same original initiator molecule, whereas cage processes of type 3 involve mainly reactions of fragments originating from different initiator molecules.

To clarify these important points, type 1 and type 2 processes can only lead to combination products of composition a + b, but the type 3 process can lead to combination products of composition a + b, a + a, and b + b.

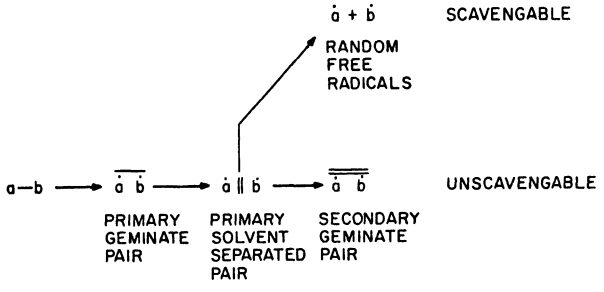

Fig. 7. Schematic representation of pathways to form primary geminate (caged) pairs, primary solvent separate pairs, secondary geminate (caged) pairs and random free radicals.

The cage effect in the reactions of radical pairs.

The "cage effect" of radical pairs is a consequence of the competition between cage processes and escape of the pair from the solvent cage. The cage effect may be rendered quantitative by making escape irreversible. Operationally, this may usually be achieved by employing free radical scavengers that efficiently react with all radicals that escape from solvent cages (Fig. 8). When the yield of cage product becomes independent of further increases in the concentration of scavenger, the unscavengable fraction of radical pairs represents the "cage effect". Note from Fig. 8 that in the absence of scavengers cage reaction occurs via both geminate radical pairs and via radical pairs produced from encounters of random free radicals.

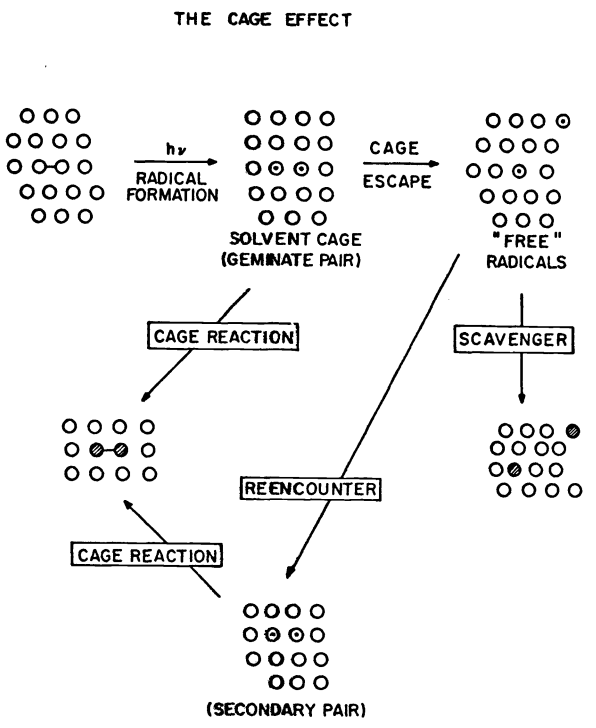

Fig. 8 Schematic representation of the cage effect in a liquid.

Micellar aggregates formed from ionic detergents in aqueous solution.
A detergent molecule typically possesses a partial hydrophobic and partial hydrophilic structure. For instance (Fig. 9) ionic detergents commonly have a straight chain hydrocarbon "tail" consisting of 10-18 carbon atoms terminating in an ionic "head". Hexadecyltrimethylammonium chloride (HDTCl) $CH_3(CH_2)_{15}\overset{+}{N}(CH_3)_3\bar{Cl}$ is an example of a cationic detergent and sodium dodecylsulfate (SDS) $CH_3(CH_2)_{11}OSO_3^-Na^+$ is an example of an anionic detergent. When added to water at low concentrations, these detergents form solutions possessing properties expected for solutions of simple electrolytes. Above a certain concentration, (that depends on the detergent structure) many of the properties (i.e., viscosity, light scattering, electrical conductance) of the solution deviate sharply from those expected for solutions of simple electrolytes (7).

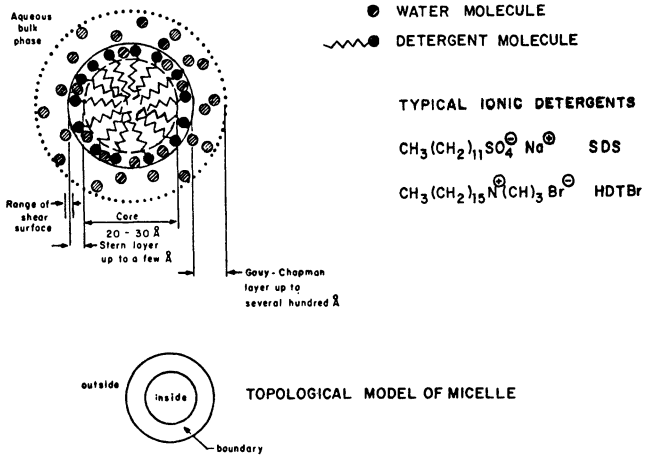

Fig. 9 Schematic model of micelle aggregates formed by addition of HDTCl or SDS to water.

The concentration (or range of concentrations) for which the properties of detergent solutions begin to show sharp deviation from the behavior of simple electrolytes is called the "critical micelle concentration" or CMC because at this concentration detergent molecules begin to aggregate to form micelles. Fig. 9 shows a schematic model of the micelle aggregates formed from HDTCl and SDS at concentrations near the CMC. We assume for simplicity that such micelles have maximal cross sections of the order of 20-30Å, which correspond to ∿50-100 detergent molecules per micelle. These micelles provide microscopic hydrophobic environments in a fundamentally aqueous medium. The important topological properties of micelles (those geometric properties which are independent of the detailed detergent structure or the detailed micelle structure) are (1) an inside which is hydrophobic and capable of solubilizing organic molecules; (2) a high polar boundary that separates the hydrophobic inside from the bulk aqueous phase and (3) an outside that consists of the bulk aqueous phase.

Micelle aggregates as hydrophobic cages for the reactions of radical pairs.
The hydrophobic interior of a micelle provides an interesting restricted volume of hydrophobic space (in an otherwise aqueous environment) that is capable of solubilizing an organic substrate. When an organic molecule enters and is solubilized by a micelle, for a certain period of time the solute is captured by the micelle. During this time period, the translational freedom of the solute is mostly restricted to the hydrophobic inside of the micelle.

Consider now a geminate radical pair that is generated by homolytic cleavage of a molecule that is solubilized in the micelle. This pair will remain geminate until one or both of the radicals escapes into the bulk aqueous phase. Thus, there is a close analogy to the ideas of a solvent cage for a homogeneous fluid solution and the hydrophobic cages provided by micellar aggregates.

In terms of the reactions of radical pairs, some important quantitative differences exist between solvent cages and micelles. The first difference has to do with the "size" of the two cages. The volume of a solvent cage, by definition is roughly the size of the encounter radical pair, i.e., very little free volume is available to the pair so that occupation of the cage is equivalent to being in the state of collision. The volume of a micellar cage, on the other hand, is large enough to allow the geminate pair to separate by distances up to tens of Å. The second difference has to do with the time scale for which the radical pair exists as a geminate pair. For non-viscous organic solutions (e.g., benzene, acetonitrile) at ambient temperature the residence time of a primary geminate pair in a solvent cage is $\sim 10^{-10}$-10^{-11} sec. In contrast, if the radical pair each possess six or more carbon atoms, the residence time of the pair in the micelle will generally be $>10^{-6}$sec.

The effect of micellization on reactions involving radical pairs.
Qualitatively there are a number of general and novel consequences expected when hydrophobic radical pairs are generated photochemically in micelle environments: (1) An increase in the efficiency of cage reactions, relative to homogeneous solution, as a result of the relatively slow escape rate of radicals from micellar cages relative to solvent cages and (2) a decrease in the quantum yield for net reaction in micelles relative to homogeneous solvents as a result of enhanced radical recombination (also a manifestation of the slower escape rate of radicals from micellar relative to solvent cages).

Consider the steps given in eqs. 2 and 3.

$$\overline{RP} \xrightarrow{k_c} \text{cage reaction} \qquad (2)$$

$$\overline{RP} \xrightarrow{k_e} \text{irreversible cage escape} \qquad (3)$$

The efficiency of cage reaction is given by

$$\text{cage reaction} = \frac{k_c}{k_c + k_e} \qquad (4)$$

and the quantum yield for net reaction is given by

$$\Phi = \phi_{1_{\overline{RP}}} (\phi_{rec.}) \left(\frac{k_c}{k_c + k_e} \right) \qquad (5)$$

where $\phi_{1_{\overline{RP}}}$ is the efficiency of producing a caged singlet radical pair per photon absorbed, and ϕ_{rec} is the fraction of singlet radical pairs that undergo regeneration of the starting material as one of the cage reactions.

In homogeneous solution triplet radical pairs undergo relatively slow ISC, whereas escape from solvent cages are relatively fast. As a result, $k_e >> k_c$ and cage effects starting from triplet pairs are small ($\lesssim$1-10%). In micelles, the slow ISC of triplets is not as crucial

since the residence time of radical pairs in the micelle cage are much longer. As a result, $k_e \lesssim k_c$ and cage effects starting from triplet pairs may be appreciable ($\lesssim$ 30-100%).

Fig. 10 summarizes schematically the important time scales pertinent to cage reactions of radical pairs in micelles. In order for hfi to be effective, the spin correlation of the radical pair must last $\sim 1 \times 10^{-7}$ to $\sim 1 \times 10^{-6}$ sec., i.e., the radical pair must remain geminate and not diffuse too far apart (lest the electron correlation be lost) during this time period. The "lifetimes" of typical organic solutes in micelles are commonly $>10^{-6}$ sec. and the dimensions of typical micelles from HDTCl and SDS prevent separation of the fragments of a radical pair by more than ~8-10Å. Thus, conditions are ideal for effective hfi induced ISC for radical pairs generated in HDTCl and SDS micelles.

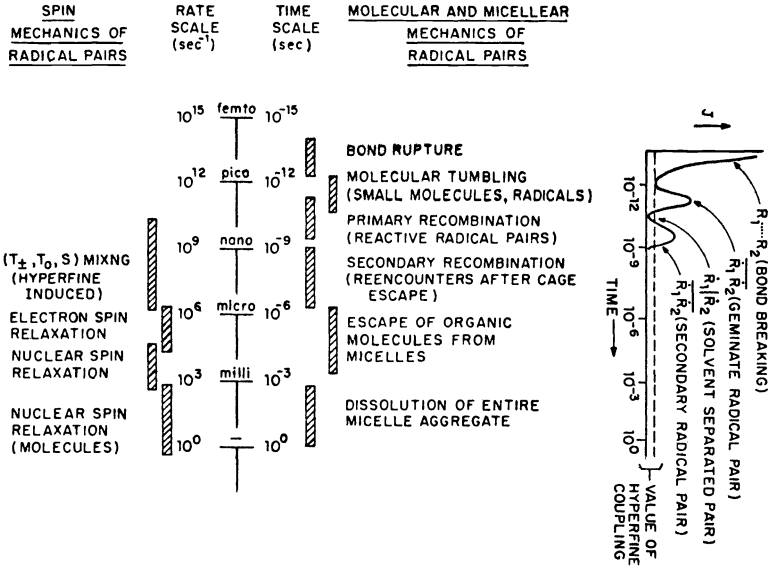

Fig. 10 Time scales for important dynamic processes involving micelles, solutes in micelles and spin dynamics.

Examples of the cage effect in micelle aggregates. Photolysis of dibenzyl ketones and substituted dibenzyl ketones.

The photolysis of dibenzyl ketone (DBK) and substituted DBK's in homogeneous solution has been shown to proceed via the following "two dot" mechanism (8):

$$C_6H_5CH_2COCH_2C_6H_5 \xrightarrow{h\nu} S_1 \rightarrow T_1 \rightarrow C_6H_5CH_2\dot{C}O + \dot{C}H_2C_6H_5 \rightarrow C_6H_5\dot{C}H_2\dot{C}H_2C_6H_5 + CO \rightarrow C_6H_5CH_2CH_2C_6H_5$$

The molecular triplet state, T_1, undergoes a primary photochemical process to produce a caged (triplet) geminate radical pair as a result of homolytic α-cleavage. Evidently cage recombination of the geminate pair is not very efficient because the quantum yield for formation of DPE is quite high (~0.7). Nevertheless, a CIDNP study (9) indicates that a small fraction of the geminate $C_6H_5CH_2\dot{C}O$ $\dot{C}H_2C_6H_5$ pair undergoes cage recombination. However, scavenging experiments (10) lead to the conclusion that the cage effect for combination of geminate $C_6H_5\dot{C}H_2\dot{C}OCH_2C_6H_5$ radical pairs is ~0. These conclusions are confirmed by experiments with asymmetrical dibenzyl ketones:

$$C_6H_5CH_2COCH_2Ar \xrightarrow[-CO]{h\nu} C_6H_5CH_2CH_2C_6H_5 + C_6H_5CH_2CH_2Ar + ArCH_2CH_2Ar$$

ACOB AA AB BB

The ratio of products AA:AB:BB would be 0:100:0 if there were 100% cage effect and 25:50:25 if there were 0% cage effect. Experimentally the ratio is very close to 25:50:25, i.e., a cage effect of ~0% is observed (11).

Cage effects are measured experimentally by two standard methods: (1) scavenging experiments in which it is shown that at sufficiently high concentration of scavenger, all non-geminate radical pairs (i.e., all the "free radicals" radicals that irreversibly escape the primary cage) are quantitatively scavengable. The cage effect is then given by the fraction of decomposed starting material that forms cage product(s) in the presence of sufficient scavenger to intercept all free radicals; (2) product ratio experiments in which the cage reactions of free radicals is known to occur in a certain fashion and the experimental ratio is then compared to a standard. For example, if an asymmetrical ketone ACOB yields products AA, AB

and BB after decarbonylation the cage effect (assuming random coupling of $\dot{A}$ and $\dot{B}$ free radicals) is given by

$$\text{cage effect} = \frac{AB-(AA + BB)}{AA + AB + BB} \qquad (6)$$

In terms of a scavenging experiment, the cage effect would be given by

$$\text{cage effect} = \frac{(AB)_{us}}{(ACOB)_R} \qquad (7)$$

where $(AB)_{us}$ is the unscavengable amount of asymmetrical coupling product and $(ACOB)_R$ is the amount of reacted ketone.

The photolysis of dibenzyl ketone (DBK) in aqueous HDTCl solution (above the CMC), results in nearly quantitative formation of 1,2-diphenylethane (DPE) and a low yield of an isomeric ketone 4-methylphenylacetophenone (PMPA) (11).

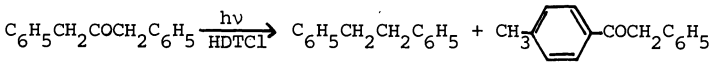

DBK DPE PMPA

Addition of $CuCl_2$ to the HDTCl solutions of DBK results in an initial lowering of the yield of DPE followed by an independence of the yield of DPE upon further addition of $CuCl_2$ (Fig. 11). New products, benzyl alcohol and benzylchloride are produced:

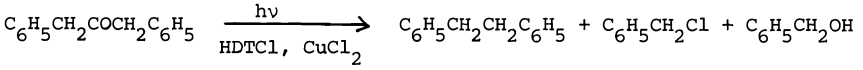

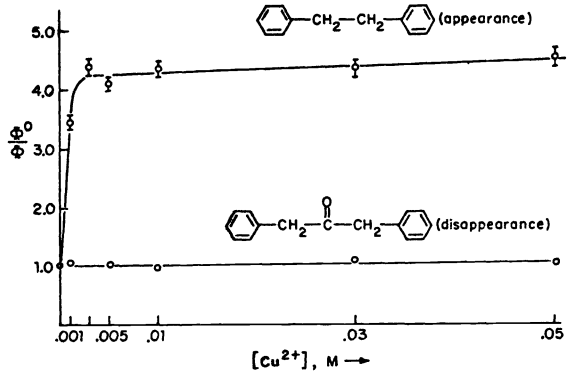

Fig. 11 The relative yield of DPE and the yield of DBK disappearance as a function of added $CuCl_2$ to HDTCl solution. Note that the yield of DPE is initially very sensitive to added scavenger but then becomes insensitive to further addition of scavenger. On the other hand, the disappearance of DBK is independent of scavenger concentration. These results are consistent with ineffective scavenging of geminate $C_6H_5CH_2\dot{C}O\ \dot{C}H_2C_6H_5$ radicals which presumably either recombine or undergo decarbonylation and do not escape from micelle cages. On the other hand, geminate $C_6H_5\dot{C}H_2\ \dot{C}H_2C_6H_5$ radical pairs undergo substantial micelle escape in competition with combination to form DPE.

Since HDTCl possesses a positively charged boundary Cu^{2+} and $CuCl^+$ (formed by solution of $CuCl_2$ in the bulk aqueous phase) will experience a strong repulsion as they approach the micellar boundary. As a result, $C_6H_5\dot{C}H_2$ radicals in micelles are protected from reaction with Cu^{2+} and $CuCl^+$. However, upon escape from the micellar to the bulk aqueous phase, $C_6H_5\dot{C}H_2$ radicals are quantitatively scavenged by aqueous phase copper ions. From the effect of copper scavenging on the yield of DPE, a cage effect of 30% may be computed from eq. 7. The situation is shown schematically in Fig. 12.

The cage effect for DBK in HDTCl may also be measured without employing a scavenger. When mixtures of $C_6H_5CH_2COCH_2C_6H_5$ and $C_6H_5CD_2COCD_2C_6H_5$ are photolyzed in HDTCl solutions (under conditions that micelles do not contain more than one DBK molecule), a mixture of isotopic DPE's is produced (12).

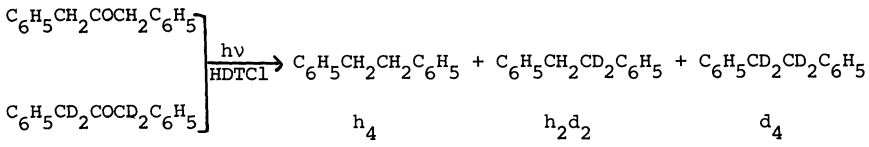

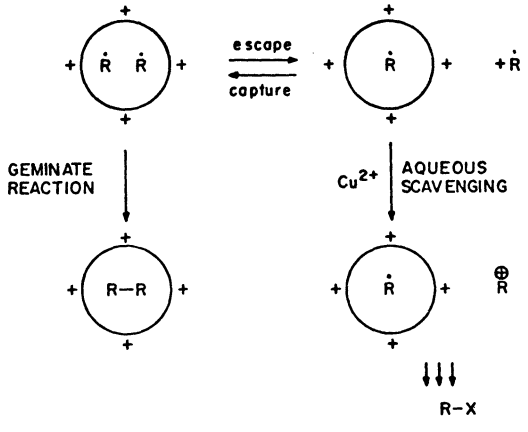

ABSENCE OF SCAVENGER:

$$\dot{R}\ \dot{R} \longrightarrow \underset{\text{(geminate)}}{R\text{-}R} + \underset{\text{(escape)}}{R\text{-}R}$$

PRESENCE OF SCAVENGER:

$$\dot{R}\ \dot{R} \longrightarrow \underset{\text{(geminate)}}{R\text{-}R} + \underset{\text{(escape)}}{R\text{-}X}$$

Fig. 12 Schematic representation of the copper scavenging experiment. Geminate radical pairs are produced in micelles. In the absence of Cu(II) scavenger, the coupling product is formed by two pathways: combination of geminate radical pairs and combination of free radicals. In the presence of sufficient Cu(II) scavenger (Fig. 11), the free radical pathway to combination product is diverted to formation of products RX, which result from scavenging.

From the yields of h_4, h_2d_2 and d_4, the cage effect may be computed from an equation analogous to eq. 6.

$$\text{cage effect} = \frac{h_4 + d_4 - h_2d_2}{h_4 + d_4 + h_2d_2}$$

Experimentally, a cage effect = 30% is obtained by this method. Since the agreement is excellent between the measured cage effects by the scavenging method and by the product ratio method, we are confident that the use of copper as a scavenger does not significantly perturb the behavior of the radical reactions occurring in micelles of HDTCl.

The dependence of the cage effect on micelle occupancy by ketones.

The question arises as to whether a second radical pair can be generated in a micelle during the lifetime of a pair that has been previously generated in the same micelle. If this should be the case, the cage effect would decrease because $\dot{A} + \dot{A}$ and $\dot{B} + \dot{B}$ combinations could now occur within the micelle cage. Experimentally, one can vary the "occupancy number" (defined as the ratio of concentration of ketone to concentration of micelles) of ketones in a micelle from values for which there is a low probability of finding more than one ketone in a micelle to values for which there is the probability of finding more than one ketone in a micelle is essentially unity.

Measurement of the cage effect as a function of occupancy number, <n>, provides information on whether more than one radical pair exists within a micelle during the same time period. Table 3 summarizes the results of such experiments (12). Variation of <n> from 0.4 to 17 leads to a variation of only a few percent in the cage effect. Thus, formation of multiple radical pairs in the same micelle during a common time period is not important. Indeed, the observed slight decrease in the cage effect at higher values of <n> may be due to an increased escape route, since it is known that addition of hydrophobic molecules to micelles causes a "loosening" of the micelle structure in addition to an increase in the size of micelles.

TABLE 3. Cage effect for 4-methylbenzyl benzyl ketone as a function of micelle occupancy number.

Ketone[a]	HDTCl[a]	<n>[b]	%Cage[c]
.0004	0.1	0.4	50
.0006	0.1	0.6	49
.001	0.1	1	50
.0025	0.1	25	47
.004	0.1	4	45
.010	0.1	10	44
.017	0.1	17	44
.002	0.1	2	48
.001	0.05	2	52
.0055	0.028	2	48

(a) Concentration in moles/liter.
(b) Ratio of [ketone]/[micelles]. An aggregation number of 100 is used to calculate [micelles].
(c) Error limits ±10% of value states; i.e., 50=50±5%. Experiments at 0 G (earth's field). Cage effect computed from eq. 6.

Magnetic field effects and magnetic isotope effects on the cage effect in micellar solution. Consider Fig. 13 which shows schematically a situation in which a triplet radical pair is generated in a micelle. Suppose that ISC to form a singlet radical pair is determined by hfi,

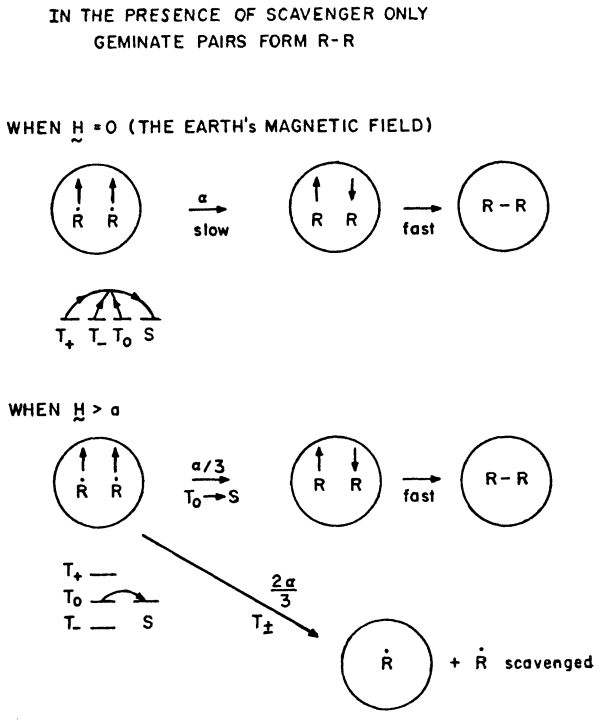

Fig. 13. Schematic representation of the influence of a laboratory magnetic field on the efficiency of the cage reaction of a triplet radical pair in a micelle. In the earth's field ISC from T_+ and T_0 to S is maximal and the fraction α of triplet radical pairs undergo cage combination. When the applied field is strong enough to inhibit $T_+ \not\rightleftarrows S$ ISC, the fraction of cage combination (in the limit) decreases to $\bar{\alpha}$ 1/3.

then at $\vec{H}$=0 G, all three triplet levels will undergo hfi ISC to S, a singlet radical pair will be formed and cage reactions (e.g., combination) will occur. When a magnetic field is applied, T_+ will be split from S and when the field is strong enough, so that only $T_o \rightarrow S$ ISC will occur. These ideas predict the following experimental consequences: (1) the cage effect will decrease as a laboratory magnetic field is improved on the sample; (2) the effect of the field will "saturate" at a few hundred G, since hyperfine interactions are generally less than 100 G. Confirmation of these expectations are shown in Fig. 14.

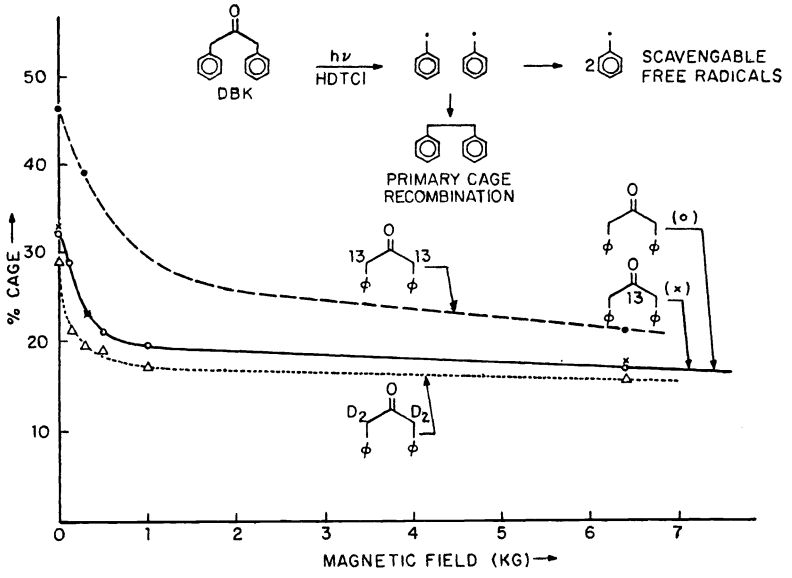

Fig. 14 Cage effects for DBK and isotopically substituted DBK's. Note that ^{13}C substitution at C-1 has no influence on the cage effect, but ^{13}C substitution at C-2,2' causes a substantial increase in the cage effect. See the text for a discussion.

Thus for the photolysis of DBK in HDTCl micelles, it can be seen that the cage effect for DBK at $\vec{H}$ = 0G, which is ∿30% drops quickly to a value of ∿20% as fields of a few hundred G are imposed on the sample, but as the field is increased from ∿500 G to ∿5000 G no further change in the cage effect occurs (13).

Fig. 14 also demonstrates a remarkable magnetic isotope effect on the extent of cage reaction, i.e., for DBK which is enriched in ^{13}C in the 2,2' positions, the cage effect is dramatically higher (46%) than it is for natural abundance DBK (31%). This result is readily understood by postulating that triplet $C_6H_5\dot{C}H_2$ $^{13}\dot{C}H_2C_6H_5$ radical pairs undergo more rapid ISC than triplet $C_6H_5\dot{C}H_2$ $\dot{C}H_2C_6H_5$ radical pairs.

Quantum yields for photolysis of dibenzyl ketone in micellar solution.
Table 4 lists the quantum yields (14) for photolysis of DBK and substituted DBK's. The quantum yield for disappearance of DBK in benzene, acetonitrile and other homogeneous organic solvents is ∿0.7. Notice the substantial drop in Φ (to ∿0.3) in micellar solution. This decrease is probably associated at least in part with a more efficient recombination of the $C_6H_5CH_2CO$ $CH_2C_6H_5$ produced by α-cleavage.

The effects of isotopic and alkyl substitution on Φ_{-k} for ketone disappearance and for the amount of scavengable diaryl ethane are notable (12). First, substitution of ^{13}C at the C-1 position leads to a decrease in Φ for net reaction, but does not lead to an increase in scavengable benzyl radicals. Consider Fig.15 for an examination of these effects. A magnetic isotope effect operates on the primary triplet $C_6H_5CH_2CO$ $CH_2C_6H_5$ pair and causes a more efficient recombination to occur for DBK-1-^{13}C relative to DBK. This leads to a decrease in Φ_{-k} for ^{13}C at C-1. After decarbonylation the triplet benzyl radical pairs are produced from DBK-1-^{13}C and DBK are equivalent, so that the quantum yield for non-scavengable diphenylethane (Φ_{+E}) and the cage effect is the same for each ketone.

On the other hand, substitution of ^{13}C at the α,α' position lead to both a decrease in Φ_{-k} and to an increase in Φ_{+E}. From Fig. 15, the decrease in Φ_{-k} is attributable to a magnetic isotope effect which leads to a more efficient recombination of C_6H_5 $^{13}\dot{C}H_2CO$ $^{13}\dot{C}H_2C_6H_5$ radi-

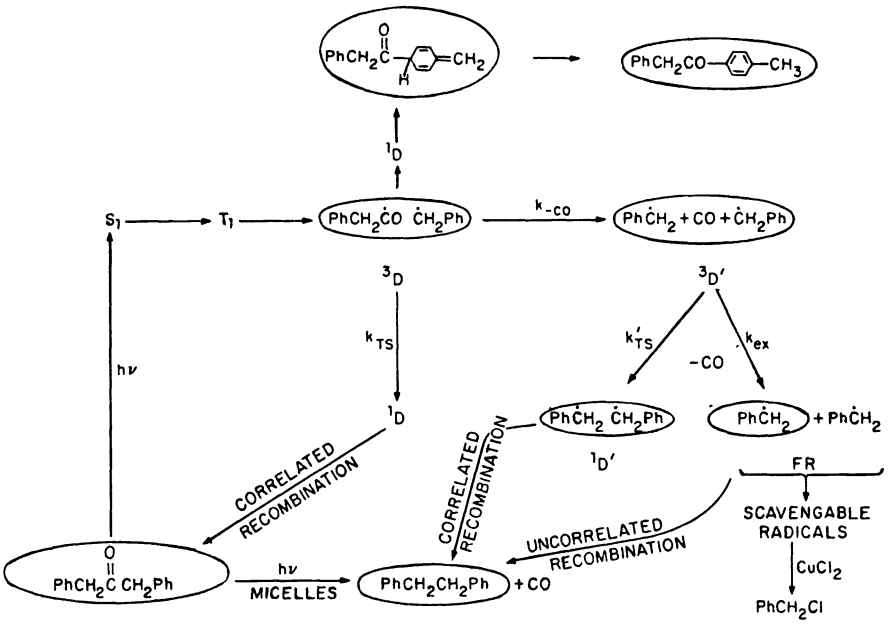

Fig. 15 Reaction scheme for discussion of magnetic effects on the photochemistry of DBK in micellar solution. The encircled species represent micellized molecules or radicals.

cals (due to more efficient ISC) relative to $C_6H_5CH_2\dot{C}O\ \dot{C}H_2C_6H_5$ radicals. Likewise, the recombination of $C_6H_5{}^{13}\dot{C}H_2\ {}^{13}\dot{C}H_2C_6H_5$ triplet radical pairs is more efficient than that of $C_6H_5\dot{C}H_2\ \dot{C}H_2C_6H_5$ radical pairs, resulting in a larger value of Φ_{+E} for DBK-2,2'-^{13}C.

In the case of DBK's that possess alkyl substituents in the 4(and4') positions, the trend is for alkyl substituents to promote lower values of Φ_{-K} and larger values of Φ_{+E}. The latter is readily understood in terms of a decreasing escape rate as the hydrophobicity of the benzyl radical is increased. The lowering of Φ_{-K} may be due to a combination of factors, including more efficient combination of geminate radical pairs before decarbonylation or a decrease in the efficiency of primary α-cleavage.

TABLE 4. Quantum yields for photolysis of dibenzyl ketones in 0.5 M HDTCl.

Ketone[a]	Φ_{-K}[b]	[Cu(II)][c] Φ_{-K}	[Cu(II)][c] Φ_{+E}	Cage Effect
DBK	0.30	0.30	0.061	33%
DBK-1-^{13}C	0.22	0.22	0.061	33%
DBK-2,2'-^{13}C	0.25	0.25	0.076	46%
4-Me-DBK	0.23	0.23	0.090	52%
4,4'-di-Me-DBK	0.16	0.16	0.085	59%
4,4'-di-t-Bu-DBK	0.13	0.13	0.12	95%

(a) [Ketone] = 0.005 M except [4,4'-di-t-Bu-DBK] = 0.0002 M.
(b) Quantum yield for disappearance of ketone. In the absence of Cu(II) the yield of diphenyl ethane(s) is nearly quantitative (>90%) for all ketones studied.
(c) Quantum yield for disappearance of ketone (-K) and for the appearance of diphenyl ethane (+E) in the presence of 0.005 M $CuCl_2$.

Enrichment in the photolysis of dibenzyl ketone.
If a HDTCl solution of dibenzyl ketone (DBK) is photolyzed to partial conversion, the residual, recovered DBK is found to be enriched in ^{13}C relative to the initial, unphotolyzed DBK. As a simple demonstration of this effect consider Figure 16 which shows the 'H NMR spectrum of DBK that has been synthetically enriched to 47.6% in ^{13}C at the carbonyl carbon (natural abundance ^{13}C is 1.1% per carbon atom) (15). A very sensitive test for the ^{13}C enrichment of the carbonyl of DBK is available by the ^{13}C satellites in the 'H-NMR spectrum: the methylene protons of DBK (Fig. 16) with a ^{12}C carbonyl are a singlet (at 3.66 ppm, $CDCl_3$, TMS as internal reference), while a doublet centered at the same chemical shift with $J_{^{13}C,H} = 6.5$ Hz is caused by ^{13}C-proton coupling when ^{13}C is contained in the carbonyl. Integration over the singlet and doublet signals allows determination of the ^{13}C content of the carbonyl of DBK with good precision and accuracy. Thus, from the "satellite method", 62 ± 4% ^{13}C is computed in the recovered DBK (after 91% conversion). For the DBK recovered after 91% conversion, a quantitative agreement exists between the mass spectrometrically determined mass increase and the 'H-NMR determined ^{13}C enrichment of the carbonyl of DBK. These samples of DBK,

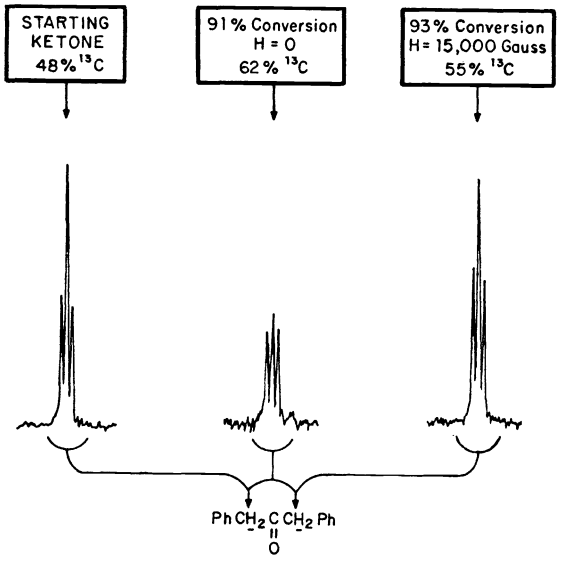

Fig. 16 'H-NMR spectra of DBK is synthetically enriched in ^{13}C at C-1. Left: CH_2 absorption of starting ketone. Middle: CH_2 absorption of DBK recovered after 91% conversion by photolysis in HDTCl solution. Right: CH_2 absorption of DBK recovered after 93% conversion by photolysis in HDTCl solution which was subjected to a field of 15,000 G.

after MS and 'H-NMR analysis were subsequently subjected to ^{13}C-NMR analysis, which also established qualitatively that the predominant ^{13}C enrichment occurs in the carbonyl of DBK (the relative increase of the carbonyl signal corresponds to a 60 ± 15% ^{13}C content). However, a small ^{13}C enrichment of the methylene carbons in ^{13}C was also apparent.

From the same experiment (DBK originally containing 47.6% ^{13}C in the carbonyl), the ^{13}C enrichment in the isomeric ketone, 1-phenyl-4-methylacetophenone (PMAP), was also determined by mass spectroscopy and 'H-NMR (satellite method, Figure 17). Both analyses demonstrated an increased content of ^{13}C carbonyl of PMAP, for a sample recovered arter 92% conversion: Mass spectral analysis (58.7% ± 2% ^{13}C) and 'H-NMR satellite analysis (57.5% ± 4% ^{13}C). Interestingly, only a small difference of the ^{13}C content of the carbonyl in PMAP is noticed, when comparing samples taken after 92% conversion (58.7%± 2% ^{13}C) or after only 29% conversion (54.4% ± 3% ^{13}C).

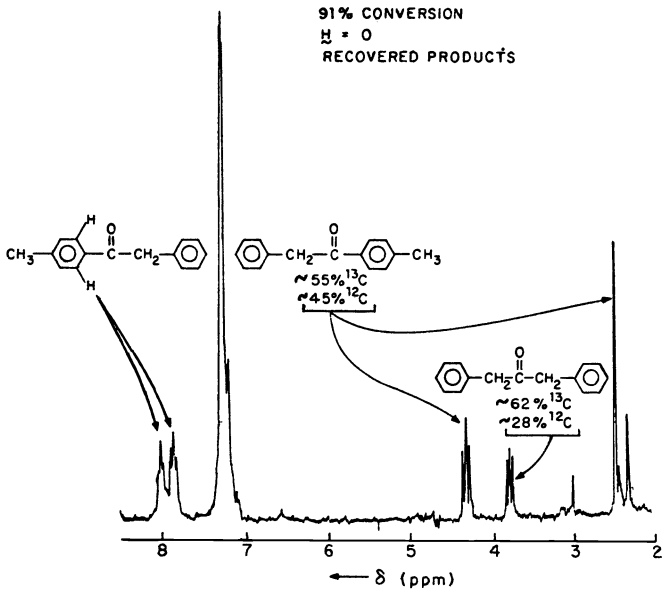

Fig. 17 'H-NMR spectrum of the residual ketone, purified by preparative VPC, after photolysis of DBK in HDTCl solution. The initial DBK possessed 48% ^{13}C at the C-1 position.

The isotope enrichment parameter, α.

Bernstein (16) has shown that for a competitive first order isotopic reaction the residual unconverted starting material becomes exponentially enriched in the slower reacting isotope. As a result, if the isotope rate factor is substantial and if the reaction is run to high conversion, the recovered material may become significantly enriched in the slower reacting isotope. In the case of the photolysis of DBK, if we consider only the $^{12}C/^{13}C$ competitive isotopic reactions, then residual, unconverted DBK will become enriched in ^{13}C, if molecules containing this isotope proceed to products at a slower rate than molecules that contain ^{12}C. The parameter α is defined as the single stage separation factor, and can be computed from the measurable quantities S, the overall separation factor (related to the ^{13}C content of product relative to starting material), and f, the fractional conversion. For practical cases the appropriate approximate formula for calculation of α is

$$\log S = \frac{\alpha-1}{\alpha} [-\log (1-f)] \qquad (9)$$

Thus, one can measure the ^{13}C content of the recovered DBK, compare it to the ^{13}C content of the initial DBK, compute S and then plot log S versus -log (1-f). The slope of such a plot, if linear, is identified as $(\alpha-1)/\alpha$. Experimental plots are shown in Figure 18 on next page.

The observation that eq. 9 is obeyed experimentally provides a useful parameter, α, for quantitative discussion of enrichment efficiency. Consideration of Figure 19 on next page allows an appreciation of the relationship of α to $^{13}C/^{13}C$ separation efficiency. As α increases, the separation factor $(^{13}C/^{12}C)_f$ increases for any given extent of reaction. For example, for 99% conversion, if α = 1.05, 1.5, 3, 6, or 20, then $(^{13}C/^{12}C)_f$ will equal 1.4%, 5%, 19%, 37%, and 50% respectively. Suppose these α values refer to enrichment at a single carbon. Then, starting with natural abundance material $(^{13}C/^{12}C)_f$ = 1/99 at 99% conversion, this carbon will possess $(^{13}C/^{12}C)_f$ = 1/1. Putting it another way, starting with a mole of natural abundance material, the amount of the pertinent carbon atom will be ∿0.01 mole and final residual material after 99% conversion (0.01 mole) will contain ∿0.005 mole of ^{13}C!

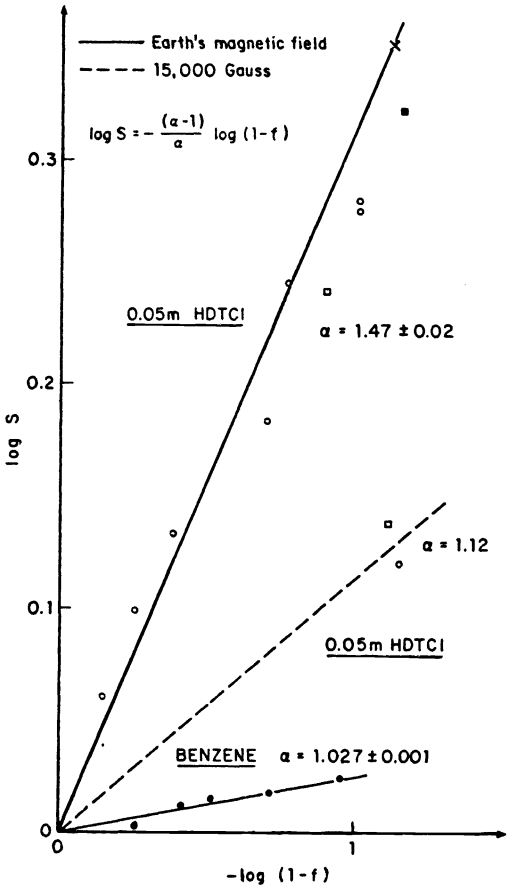

Fig. 18 Typical experimental plots of log S versus -log (1-f) for the photolysis of DBK in HDTCl solution.

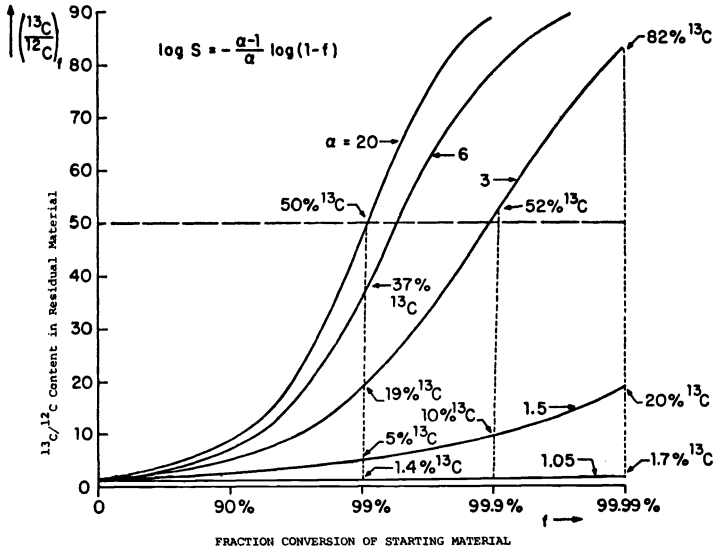

Fig. 19 Relation of experimental ^{13}C enrichment (calculated for a single carbon atom) as a function of conversion for the photolysis of DBK. The family of curves are generated by employing different values of α in eq. 9.

The relationship of α to isotope separation efficiency and to magnetic resonance parameters. The electron spin resonance (ESR) spectra of both the $PhCH_2\dot{C}O$ and the $\dot{C}H_2Ph$ radicals have been obtained in homogeneous fluid solution (Fig. 20). Nearly all of the lines in this spectrum arise mainly from proton-electron interactions. From the splittings shown in the figure, the values of ^1H_a, the hyperfine coupling constants for protons and the odd electron of the benzyl radical have been extracted and are listed in Figure 21. It is possible to use

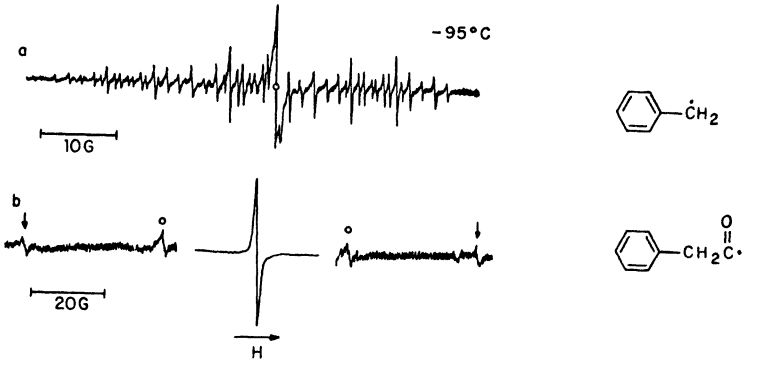

Fig. 20 ESR spectra of $C_6H_5\dot{C}H_2$ and $C_6H_5CH_2\dot{C}O$ produced by photolysis of DBK at -95°C. Ref. H. Paul and H. Fischer, Helv. Chim. Acta, 56, 1575 (1973).

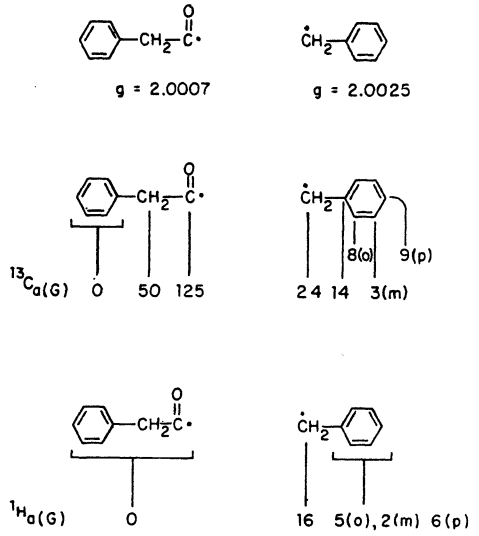

Fig. 21 ESR parameters of the $C_6H_5\dot{C}H_2$ and $C_6H_5CH_2\dot{C}O$ radicals. Ref. A. Berndt, H. Fischer and H. Paul, "Magnetic Properties of Free Radicals," Londolt-Bornstein, vol. 9, part b, Springer-Verlag, Berlin, 1977: $PhCH_2$, p. 543; $PhCH_2\dot{C}O$, p. 321. The values for ^{13}C coupling of the benzene ring of $C_6H_5\dot{C}H_2$ are estimated from spin densities of the benzyl radical and measured proton hfc according to M. Karplus and G.K. Fraenkel, J. Chem. Phys., 35, 1312 (1961) employing data from A. Carrington and I.C.P. Smith, Molec. Phys., 9, 137 (1965).

an ESR saturation technique to wipe out the $PhC\dot{H}_2$ spectrum, but preserve the $PhCH_2\dot{C}O$ spectrum. The much simpler resulting spectrum (Figure 20) shows that proton-electron hyperfine coupling is negligible in the $PhCH_2\dot{C}O$ radical, since the spectrum at low gain shows only a single line (center line of Fig. 20). At high gain additional lines appear, due to ^{13}C hyperfine coupling. Only the ^{13}CO carbon and the $^{13}CH_2$ carbon atoms are significantly coupled to the odd electron of the $PhCH_2\dot{C}O$ radical; however, the values of $^{13}C_a$ are much larger than nearly any known value of $^{1}H_a$.

The values of $^{13}C_a$ have been measured experimentally for the $PhC\dot{H}_2$ radical only at the CH_2 position and the ipso position. The values of $^{13}C_a$ for the ring carbons can be estimated, however, and are listed in Figure 21.

Under the simple assumption that the theoretical enrichment at a given carbon atom of DBK is proportional to the value of $^{13}C_a$ for that carbon, one can predict a rough estimate of the observed enrichment. The result is shown in Figure 22, and is quite remarkable. For a

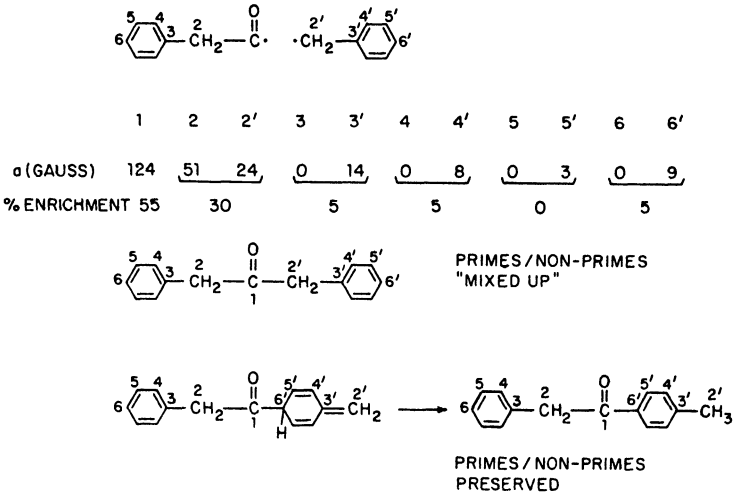

Fig. 22 Correlation of ^{13}C hyperfine coupling constants and relative enrichments at various carbon atoms for the photolysis of DBK.

single cycle, enrichment at C_1 should be ∿ 55%, and at C_2 (plus $C_2{}^1$) should be ∿30%. Minor, but potentially measurable enrichment should occur at the ring carbon atoms. The expectation that the C_1 and C_2 atoms of the residual DBK are substantially enriched was experimentally confirmed by photolyzing DBK (natural abundance) in HDTCl solution to ∿90% conversion. The residual DBK was then subjected to ^{13}C NMR analysis. Integration of the various absorption bands showed that, compared to natural abundance DBK, the enrichment of recovered residual DBK was predominantly at the C_1 and C_2 positions (17).

When the $PhC\dot{H}_2$ and $PhCH_2\dot{C}O$ radical pair combine, the C_6H_5 carbon atoms, which are distinct in the radical pair, become scrambled and equivalent in the regenerated $PhCH_2COCH_2Ph$ molecule. Thus, analysis of the residual DBK cannot reveal whether an astounding prediction of the $^{13}C_a$ values is correct, i.e., that there will be no ^{13}C enrichment of the C_6H_5 ring atoms of the $PhCH_2\dot{C}O$ moiety ($^{13}C_a = 0$ for this radical), but that there will be a (potentially measurable) ^{13}C enrichment of the C_6H_5 ring associated with the $PhC\dot{H}_2$. The occurrence of PMAP of a minor product of photolysis of DBK in HDTCl solution, provides an experimental means of testing this prediction. PMAP is presumably formed by the mechanism shown in Figure 15. When a $PhCH_2\dot{C}O$ adds to the 4 position of the $PhC\dot{H}_2$ radical, the distinctness of the C_6H_5 carbon atoms that exists in the radical pair is preserved in the primary product and the isolated product, PMAP. Thus, ^{13}C NMR analysis of PMAP should allow an experimental text of the prediction of non-enrichment of C_6H_5 ring derived from the $PhCH_2\dot{C}O$ radical. Such experiments are in progress (18).

A Schematic interpretation of isotope enrichment by the magnetic isotope effect.
The general idea behind the enrichment experiment may be understood by using a very simple schematic description of the behavior of molecules on a dissociative triplet surface which possesses a bonding singlet surface of lower energy. Figure 23 shows (left) a representative point moving along a dissociative triplet surface. The triplet surface is repulsive for all nuclear geometries corresponding to the molecular structure, i.e., in the triplet state the energy of the molecule decreases as bond a-b increases in length. We say that in the triplet state the representative point moves spontaneously to the right. Eventually,

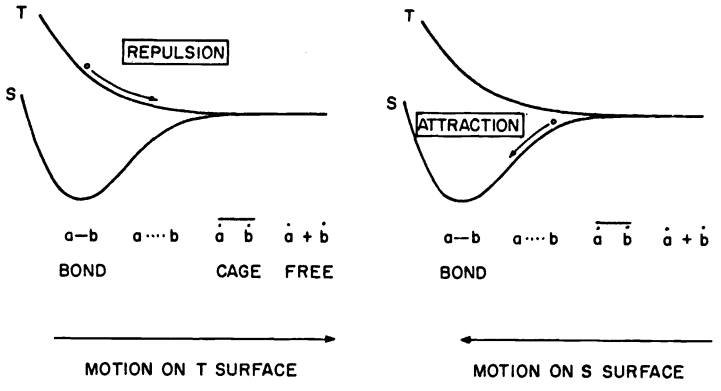

Fig. 23 Motion of a representative point on a dissociative triplet surface (left) and on an attractive singlet surface.

the bond breaks, $\dot{a}$ and $\dot{b}$ are produced and the further separation of the a and b nuclei does not lead to a further lowering of the energy of the system. Suppose that the radical pair $\dot{a}$, $\dot{b}$ can experience a mechanism that allows the representative point to "jump" to the singlet surface; once on the singlet surface the point will move spontaneously "to the left", i.e., the a-b bond will reform.

The key idea behind the magnetic isotope method for separation of ^{13}C from ^{12}C by photolysis of DBK, is the postulate that ^{13}C hyperfine coupling provides the radical pairs ($a = PhCH_2\dot{C}O$, $b = Ph\dot{C}H_2$) possessing ^{13}C with a mechanism by which the representative point can jump from the triplet surface to the singlet surface when the point is in a region for which the singlet and triplet states are degenerate. Since this mechanism is unavailable to radical pairs that possess only ^{12}C nuclei, the representative points for these molecules will not be able to make the jump from the triplet surface to the singlet surface. In effect, ^{13}C electron hyperfine coupling provides a "hole" in the triplet surface through which the ^{13}C containing triplet radical pair can jump to the singlet surface, i.e., undergo intersystem crossing from a triplet radical pair to a singlet radical pair.

Figure 24 summarizes these ideas in a highly schematic fashion. We imagine that we start with a system containing both ^{13}C containing molecules (representative points: closed circles) and ^{12}C containing molecules (representative points: open circles). Photochemical

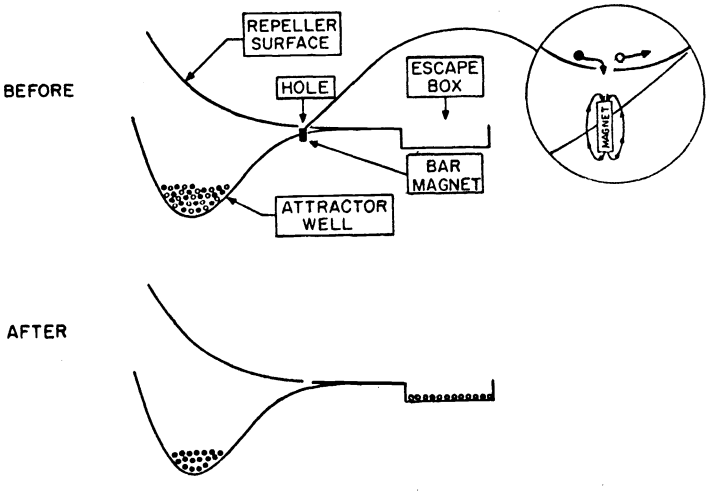

Fig. 24 Highly schematic representation of the mechanism of ^{13}C enrichment in the photolysis of DBK in HDTCl micelles.

excitation carries the points from the singlet surface to the triplet surfaces (e.g., $S_0 \rightarrow S_1 \rightarrow T_1$. Once on the triplet surface the representative points for molecules associated with

both isotopes move to the right. The closed circles find a pathway to the ground singlet surface at the "hole" provided by ^{13}C hyperfine coupling. The momentum of the non-magnetic representative points carries them past the hole into an "escape box", i.e., the formation of scavengable free radicals. The hyperfine interaction may be viewed as being analogous to a bar magnet that attracts the "magnetic" representative points through the hole. Perhaps more appropriately, the interaction may be viewed as the action of an electromagnet under the hole. This microscopic electromagnet is powered by electron motions in the radical pair, i.e., the magnitude of the hyperfine interaction varying with time as the electronic motion and distribution vary with time.

The ideas employed in the DBK system are summarized schematically in Figure 25 in terms of potential energy surfaces. The reaction coordinate represents breaking of the $OC-CH_2$ bond.

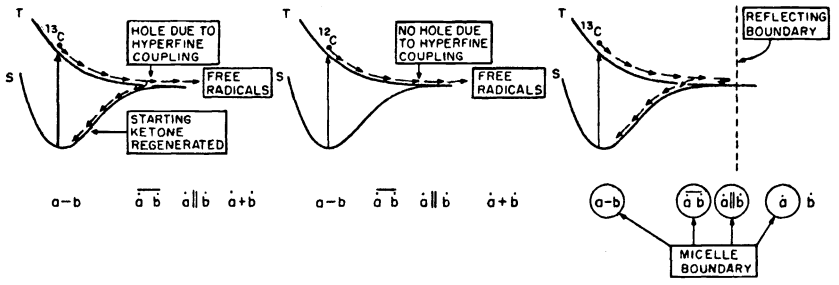

Fig. 25 Schematic representation of the effect of photolysis in micelles on the ^{13}C enrichment of DBK. In the figure a = $C_6H_5CH_2CO$ and b = $CH_2C_6H_5$.

As the $OC-CH_2$ bond breaks the point "slides" down the electronically repulsive triplet surface. When the bond is broken the triplet surface becomes essentially degenerate with the ground state singlet surface. A magnetic interaction is required before the representative point can make a "jump" from the T surface to the S surface. Such a jump can be induced by hyperfine interaction only when the point is far to the right, i.e., when the triplet and singlet are nearly degenerate and J < a. The "jump" from T to S requires a "hole" in the T surface, through which the point may fall.

The role of the micelle may be viewed as providing a boundary which "reflects" the representative point back toward the hyperfine induced hole after an "overshoot" has occurred. Thus, diffusive escape is temporarily thwarted and a ^{13}C containing molecule receives extra chances to find a hole which allows return to ground state DBK. Eventually, of course, escape by decarbonylation will take place if neither diffusive escape nor bond formation occur.

Photochemistry of 1,2-diphenyl-2-methylpropanone in homogeneous and in micellar solutions. The products of the photolysis of dibenzylketone are essentially the same for homogeneous organic solvents or for aqueous detergent solutions, since upon decarbonylation the benzyl radicals produced inevitably lead to DPE (in the absence of scavenger). In contrast, the photochemistry of 1,2-diphenyl-2-methylpropanone (DPMP) depends significantly upon the solvent environment (19). For example, photolysis of DPMP in CH_3CN leads to formation of styrene (ST) and dicumyl (DC) as the major products, with benzil and benzaldehyde formed as minor products. In micellar solution (e.g., HDTCl or SDS) the major products, in equal yields are styrene and benzaldehyde. Dicumyl is not formed in detectable amounts.

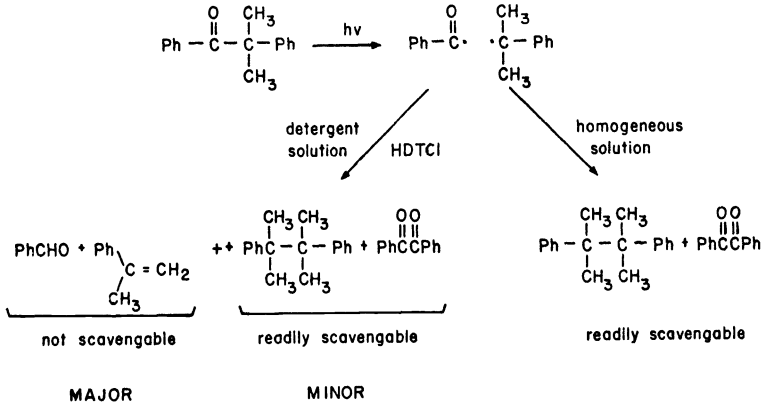

As in the case of dibenzyl ketone, the cage effect for photolysis of DPMP in micellar HDTCl solution may be computed from Cu(II) scavenging experiments. In fact, addition of Cu(II) does not affect the yield of C_6H_5CHO or of $C_6H_5C(CH_3)=CH_2$ produced. Thus, the yield of either of these disproportionation products (since the compounds are produced in equal yield), based on starting ketone consumed, equals the cage effect. The cage effects for DPMP and some of its isotopically substituted derivatives are given in Table 5.

TABLE 5. Cage effect on the photolysis of $C_6H_5COC(CH_3)_2C_6H_5$ in HDTCl solution.

KETONE	CAGE EFFECT (a)	
	0 Gauss	1000 Gauss
$C_6H_5COC(CH_3)_2C_6H_5$	30	20
$C_6H_5COC(CD_3)_2C_6H_5$	23	13
$C_6H_5{}^{13}CO(CH_3)_2C_6H_5$	42	30

(a) The cage effect is defined as the % yield of C_6H_5CHO or $C_6H_5C(CH_3)=CH_2$ produced, based on starting material consumed.

Several aspects of the data in Table 5 warrant comment: (1) the cage effect is strikingly dependent on the isotopic composition of the ketone; (2) the cage effect decreases substantially when photolysis is conducted in a magnetic field of 1000 G (the major portion of the decrease occurs at fields strengths lower than 500 G); (3) deuterium substitution (CH_3 groups) decreases the cage effect; (4) carbon-13 substitution (CO carbon) increases the cage effect. These results are all qualitatively understandable in terms of the theory of magnetic isotope and magnetic field effects on correlated radical pairs.

First we postulate (Figure 26) that in each case photolysis proceeds via T_1 which cleaves to

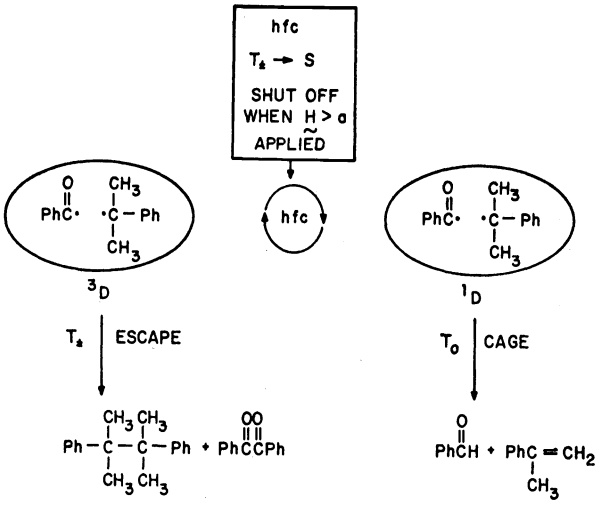

Fig. 26 Mechanism for the influence of an applied magnetic field on the photolysis of DPMP in HDTCl solution. See text for discussion.

produce a spin correlated triplet micelle caged radical pair $^3\overline{RP}$. This pair undergoes hyperfine induced ISC to eventuate in a singlet radical pair $^1\overline{RP}$ that undergoes disproportionation to C_6H_5CHO and $C_6H_5C(CH_3)=CH_2$. Escape of radicals from micelles competes only weakly for the parent ketone whose isotopic composition corresponds to natural abundance. In this case, ISC occurs mainly by the 'H induced hfi of the methyl groups of the $C_6H_5\dot{C}(CH_3)_2$ radical. Deuterium substitution decreases the rate of ISC for $^3\overline{RP}$ because of the weaker hfi of the $C_6H_5\dot{C}(CD_3)_2$ radical. Substitution of ^{13}C from ^{12}C at the carbonyl carbon of the $C_6H_5\dot{C}O$ radical introduces a new and important hfi, i.e., the large (~125 G) hyperfine interaction of a single ^{13}C is as significant as the summation of proton hfi.

The magnetic field effect in which the cage effect decreases with increasing field strength, is readily interpreted in terms of splitting of T_+ and T_- of $^3\overline{RP}$ from S and consequent decrease in the rate of $^3\overline{RP} \rightarrow {}^1\overline{RP}$. Since the rate of escape from the micelles is field

independent, the net cage effect is reduced.

The combination of isotope and magnetic field effects allow a variation of >300% in the degree of cage reaction!

Enrichment in "restricted spaces" and other micelles

Are micelles unique as vehicles for unusually large magnetic effects on radical reactions? We think not, since similar effects have been observed when the photolysis of DBK is conducted in polymer films (i.e., polymethylmethacrylate) or in porous glass. It thus appears that the radical pair is constrained to a certain "restricted space" such as that provided by micelles, the fluid portions of polymer films or the cavities of porous glass.

Magnetic isotope and magnetic field effects on the formation of singlet oxygen from thermolysis of endoperoxides.

The thermolysis of certain endoperoxides of aromatic compounds produces molecular oxygen quantitatively (20). From a study of activation parameters it has been found that these reactions proceed via two pathways (21): (1) a concerted mechanism in which $^1O_2$ is produced quantitatively and (2) a diradical maechanism in which both $^3O_2$ and $^1O_2$ are produced. Magnetic field and magnetic isotope effects potentially provide a novel and convincing tool for distinguishing concerted and diradical mechanisms. Only the diradical pathways will be influenced by magnetic effects. For example, consider the simplified diradical mechanism for endoperoxide thermolysis shown in Figure 27. If thermolysis leads initially to a singlet diradical, ^1D, this species may undergo either ISC to ^3D (path b) or fragmentation of $^1O_2$

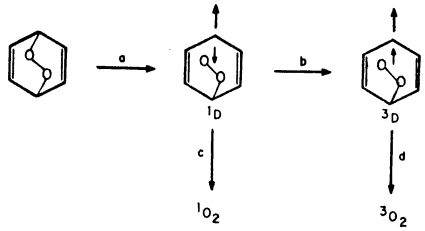

Fig. 27 Simplified diradical mechanism for the thermolysis of endoperoxides.

(path c). As in the case of radical pairs, magnetic fields may influence reactions of diradicals via a Δg effect or via a hyperfine effect. The Δg effect will increase the rate of step b relative to step c, thereby producing ^3D with greater efficiency, hence, a higher yield of $^3O_2$ and a lower yield of $^1O_2$ is expected when endoperoxides (which decompose via diradicals) are thermolyzed in a magnetic field. Furthermore, no effect of external magnetic field is expected if a concerted decomposition occurs. Figure 28 shows a plot of the $^1O_2$ yield versus H for a 1,4-endoperoxide that undergoes concerted thermolysis and a 9,10-endoperoxide that undergoes thermolysis via a diradical (21). It is extremely gratifying to find that there is no magnetic field effect on the $^1O_2$ yield for thermolysis of 1, but that a striking decrease in the yield of $^1O_2$ is observed for 2 as for variation of field strength in the range 9000-15,000 Gauss.

A spectacular prediction can be made concerning magnetic isotope effects on the thermolysis of endoperoxides: If a diradical pathway (Fig. 27) is followed, diradicals possessing ^{17}O atoms will have a higher probability of following path b than diradicals possessing only ^{16}O and ^{18}O atoms, because ^{17}O is a magnetic isotope, but ^{16}O and ^{18}O are non-magnetic isotopes. Experimentally this means that endoperoxide molecules which contain ^{17}O will produce $^1O_2$ less efficiently and $^3O_2$ more efficiently. Thus, if a selective and efficient trap of $^1O_2$ is present during reaction, the "untrappable" molecular oxygen will be enriched in ^{17}O!

To test the validity of these ideas, two types of measurements were made (22): (a) the ^{17}O and (^{16}O + ^{18}O) content of untrappable molecular oxygen was analyzed by mass spectrometry and (b) the yield of trapped $^1O_2$ was evaluated by quantitative determination of the amount of reacted acceptor when DPA-$^{16}O_2$, DPA-$^{18}O_2$ or DPA-$^{17}O_2$ ^{16}O were employed. It was found that the yield of $^1O_2$ formation is smaller for ^{17}O than for ^{16}O or ^{18}O continuing DPA-O_2. Furthermore, it was found that both DPA-^{16}O and DPA-^{18}O produce the same yield of $^1O_2$, while DPA-^{17}O produces less $^1O_2$. This result rules out a significant mass isotope effect as the basis for different quantum yields.

Since the amount of reacted trap is monitored in the yield measurements they only provide an indirect test of the isotopic enrichment. A direct measurement involves determination of the isotopic composition of the untrappable molecular oxygen produced in the thermolysis of

DPA-O_2. The results demonstrate that the untrappable molecular oxygen is indeed enriched in ^{17}O relative to the control sample (22).

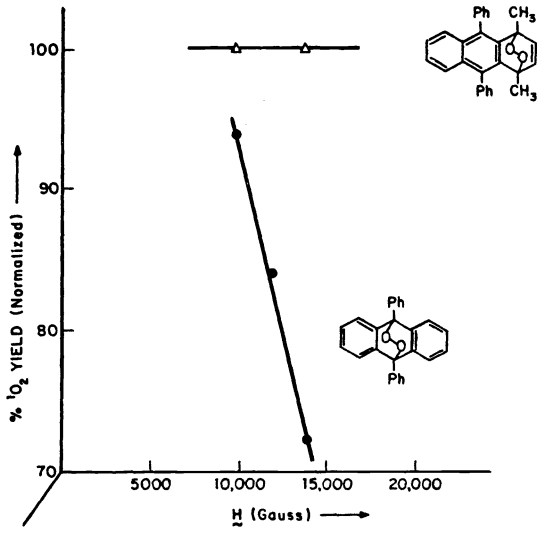

Fig. 28 Magnetic field effects on the thermolysis of a 9,10 and a 1,4 endoperoxide. See text for discussion.

In the case of ^{17}O enrichment, the hyperfine interaction provides a surface avoiding (Fig. 29, right) for ^{17}O containing diradicals where a surface crossing exists (Fig. 29, left) for ^{16}O or ^{18}O containing diradicals (23).

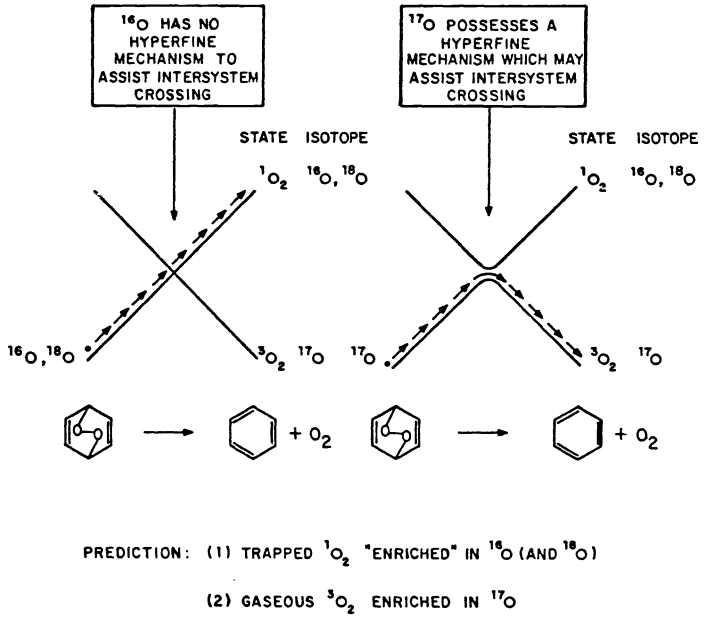

Fig. 29 Schematic surface representation of mechanism for enrichment of ^{17}O via the thermolysis of endoperoxides.

CONCLUSION

The experiments described in this report leave little room for doubting the importance of magnetic effects on the reactions of radical pairs, especially when the reactions occur in micellar cages. By appropriate manipulation of reaction condition and reactant structure, cage effects approaching 100% may be achieved for triplet radical pairs, magnetic isotopes may be separated from non-magnetic isotopes and weak magnetic fields can affect the extent of cage reactions.

The key features are the requirement of a singlet-triplet crossing (or touching) along the reaction coordinate, the availability of a hyperfine hole at the molecular geometry corresponding to the hole and sufficient time for the representative point to find the hole when it arrives in the region of "phase space" corresponding to the hole. Magnetic field and magnetic isotope effects provide a complement to CIDNP for probing mechanisms of radical reactions. In contrast to CIDNP which requires NMR measurement during reaction, magnetic field and magnetic isotope effects reveal themselves in terms of chemical products which may be analyzed at the chemist's convenience by conventional methods. It should be also noted that unusual isotope effects, that have been interpreted in terms of conventional mass effects, should be reconsidered as possible magnetic isotope effects and subjected to the magnetic field criterion.

The discovery of systematic relationships between molecular structure and chemical reactivity has been a major activity of physical organic chemists. The "two dot" representation of radical pair and diradical reactions does not possess enough "structure" to allow an understanding of the magnetic effects on cage reactions. However, the inclusion of "structural features" such as spin correlation (singlets and triplets), triplet sublevels, electron spin and nuclear spin interactions and electron spin-laboratory magnet interactions, allows for a useful qualitative framework for systemization and prediction.

Acknowledgements.
The author thanks the National Science Foundation, the Air Force Office of Scientific Research, and the Department of Energy for their generous support of this research. He is especially grateful for the outstanding experimental scientific and intellectual contributions of two collaborators, Dr. Bernhard Kraeutler and Dr. Ming-Fea Chow which form the basis of the research of this report. Professor Richard Bernstein receives a special acknowledgement for alerting us to the exceptionally useful concept of α as a parameter to systematize and to correlate our data.

REFERENCES

1. G.E. Dunn, "Isotope Effects in Organic Chemistry," vol. 3., E. Buncel and C.C. Lee, Eds., Elsevier, New York, 1977, p. 1.
2. Reviews of magnetic effects on chemical reactions: (a) P .W. Atkins and T.P. Lambert, Ann. Rep. Chem. Soc. A, 67 (1975); (b) R.Z. Sagdeev, K.M. Salikhov and Y.M. Molin, Russ. Chem. Rev., 46, 297 (1977); (c) A.L. Buchachenko, Russ. Chem. Rev., 45, 375 (1976); R.G. Lawler and G.T. Evans, Ind. Chim. Belg., 36, 1087 (1971); (d) P. Atkins, Chem. Brit. 214 (1976); (e) A.L. Buchachenko, Russ. J. Phys. Chem., 51, 1445 (1977); (f) A.L. Buchachenko, Russ. Chem. Rev.,45, 761 (1976).
3. Reviews of the theory of CIDNP: (a) R. Kaptein, Adv. Free Radical Chem., 5, 381 (1975); (b) G. Closs, Proc. Int. Congr. Pure Appl. Chem., 23rd, 4, 19 (1971); (b) A.L. Buchachenko and F.M. Zhidomirov, Russ. Chem. Rev., 40, 801 (1971); (d) P.G. Firth and K.A. Mc Lauchlan, Ann. Rep. Chem. Soc. A., 378 (1975).
4. For a review of the vector model of electron spin as applied to an understanding of intersystem crossing in radical pairs, see H.R. Ward, Acc. Chem. Res., 5, 18 (1972), and R. Kaptein, "Chemically Induced Magnetic Polarization," L.T.Muus, ed., D. Reidel, Dordrecht, Netherlands.
5. J. Frank and E. Rabinowitch, Trans. Farad. Soc., 30, 120 (1934); E. Rabinowitch and W. Wood, ibid., 32, 1381 (1936).
6. R.M. Noyes, J. Am. Chem. Soc., 77, 2042 (1955); ibid., 78, 5486 (1956).
7. J.H. Fendler and E.J. Fendler, "Catalysis in Micellar and Macromolecular Systems", Academic Press, New York, 1975.
8. P. S. Engel, J. Am. Chem. Soc., 92, 6074 (1970).
9. B. Blank, P.G. Menitt and H. Fischer, Proc. Int. Congr. Pure Appl. Chem., 23rd, 4, 1 1971.
10. W.K. Robins and R.H. Eastman, J. Am. Chem. Soc., 92, 6076 (1970).
11. N.J. Turro and W.R. Cherry,J. Am. Chem. Soc., 100, 7431 (1978).
12. G. Weed, M.-F. Chow, C.J. Chung, Columbia University, unpublished results.
13. N.J. Turro, M.-F. Chow, C.-J. Chung, G.C. Weed and B. Kraeutler, J. Am. Chem. Soc., 102 4843 (1980).
14. N.J. Turro, B. Kraeutler and D.R. Anderson, J. Am. Chem. Soc., 101, 7435 (1979).
15. N.J. Turro and B. Kraeutler, J. Am. Chem. Soc., 100, 7432 (1978).
16. R.B. Bernstein, J. Phys. Chem., 56, 893 (1952); Science, 126, 119 (1957).
17. B. Kraeutler, D.R. Anderson and N.J. Turro, unpublished results.
18. R. Lawler, G. Lehr and N.J. Turro, unpublished results.
19. N.J. Turro and J. Mattay, Tetrahedron Letters, 21, 1799 (1980).
20. J. Rigaudy and J.J. Basselier, Pure Appl. Chem. 1, 383 (1971).
21. N.J. Turro, M.-F. Chow, and J. Rigaudy, J. Am. Chem. Soc., 101, 1300 (1979).
22. N.J. Turro and M.-F. Chow, J. Am. Chem. Soc., 102, 1190 (1980).
23. N.J. Turro and M.-F. Chow, J. Am. Chem. Soc., 101, 3701 (1979).